Model study of a freshwater infiltration experiment in an ancient creek ridge in the province of Zeeland, the Netherlands.

Thomas Boerman
Student No. 3361217

September 30, 2013

Master program:
MSc. Earth, Surface and Water; track Environmental Hydrogeology

Supervisors:
Esther van Baaren (Deltares)
Pieter Pauw (Deltares)
Prof. Dr. Ruud Schotting (Utrecht University)

Universiteit Utrecht

Deltares
Enabling Delta Life

Abstract

Sea water intrusion and land subsidence are common problems in coastal areas, which are expected to increase due to the effect of climate change in the near future. In the province of Zeeland in the Netherlands, agriculture already suffers from the saline groundwater and the ongoing salinization will increase the stress on agriculture even more in the future. Freshwater lenses in creek ridges are one of the possibilities for farmers to sustain their fresh water need for irrigation. As part of the 'Knowledge For Climate' program, a field test has been set up in the project GO-FRESH with the goal of increasing the size of the freshwater lens in a creek ridge in Zeeland. The field test is done on the properties of two farmers near Serooskerke, Walcheren. The implementation of a controlled drainage system allows the farmers to infiltrate excess water into the creek ridge in the winter periods. This will raise groundwater levels in the creek ridge which results in a lowering of the freshwater-saltwater interface due to buoyancy effects. The excess water can then be pumped up again during dry periods in summer when it is most needed. The project is a collaberation between research institutes, the government and several farmers.

A 3D-density dependent groundwater model with coupled salt transport (SEAWAT) is made with the goal of predicting the short and long time effects of (1) the implementation of the drainage system and (2) climate change. The model is a detailed tool for modeling effects groundwater and depth to the fresh-brackish-saline interface. First, the current day situation without infiltration was modelled from initial saline conditions. The model has been calibrated with different measurements (hydraulic head measurements, concentration from sample analysis etc). The model gives good results for predictions on long time scales. and is therefore useful for predicting longtime effects. The implementation of the controlled drainage system will increase the size of the freshwater lens by at least 10 m (100 % increase), which is more then enough to compensate the volumetric loss of freshwater by climate change.

The same model has been used by Visser [Visser, 2012] to model freshwater lens growth on the creek ridge, but in his study another groundwater code MOCDENS3D is used, which is numerically similar to SEAWAT, but in MOCDENS3D the user is limited in the solver methods, while in SEAWAT several options are available. The differences between running the model in MOCDENS3D or SEAWAT in terms of accuracy are negligible, but in terms of runtime, MOCDENS3D is faster. On the other hand, SEAWAT is more versatile, since the possibility of modelling multiple species simultaniously can be beneficial.

Contents

List of Figures

1. Introduction

1.1 Problem statement

The province of Zeeland is located in the South-Western part of the Netherlands. Large areas in this delta are situated below mean sea level (NAP, *Normaal Amsterdams Peil*, the reference level for the Netherlands). Land in Zeeland is predominantly used for agriculture. Agriculture in the lower parts of the Netherlands is under increasing pressure by the effects of climate change in the near future. While precipitation in the winter months would cover the need for fresh water, at the time fresh water is needed the most, in the summer months, precipitation is much to low to cover the need. Access to fresh groundwater is limited; both by natural availability and permit limitations. The fresh water - salt water interface (*fresh-salt interface*) is found at a varying depth of just a meter in the lowest parts of the province up to 100 m in the dune areas [van Baaren et al., 2012]. The change in climate results in increasing sea level, increasing seepage flux, changes in precipitation and evaporation etc. This can increase crop damage caused by drought and/or salinization which would reduce profit made by farmers.

Figure 1.1.1: The Netherlands, with the province of Zeeland boxed (Source: *Google Earth*)

Figure 1.1.2: The province of Zeeland, with the field site boxed (Source: *Google Earth*)

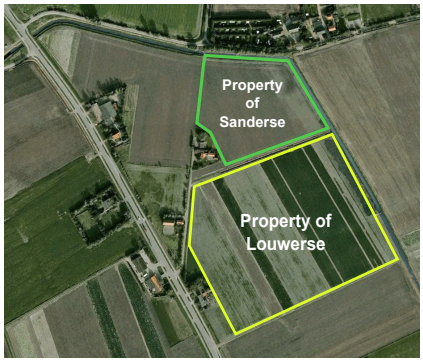

Figure 1.1.3: Properties of Sanderse and Louwerse (Source: *Google Earth*)

A possibility for sustaining the fresh water need by farmers is to pump water from freshwater lenses which have formed in ancient creek ridges. Ancient creek ridges are old sand deposits in tidal-influenced creeks. Since the creeks ran through an overall peat landscape and oxidation of the peat has occurred during the last thousands of years, the creek deposits are slightly elevated (1-3m) compared to the surrounding area, small elevation changes can be found in Zeeland (figure 1.1.4). As part of the 'Knowledge for Climate' research program, a pilot study (*GO-FRESH*) has started on the properties of two farmers, Werner Louwerse and Johan Sanderse whose properties are located directly on a creek ridge (figure 1.1.3). One farmer already pumps up fresh groundwater, but permit limitations limit the amount of water which is allowed to pump up. The volume of water which is allowed to be pumped up is based on the depth of the fresh - salt interface. If the interface could be lowered, they would be allowed to pump up more. The properties of Louwerse and Sanderse are used as a pilot study of using a *level-controlled drainage system* (explained in section (4.1)) for storing excess fresh water by precipitation combined with water from a fresh-water ditch in the creek ridge in the winter months. Excess stored water can then be pumped up when needed in the summer months.

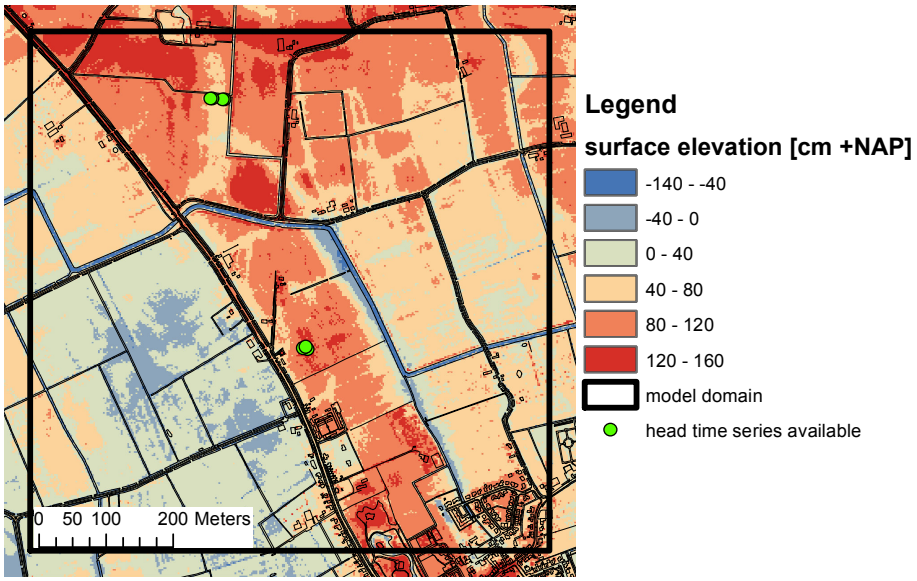

Figure 1.1.4: Surface elevation map of field site. Elevations are relative to NAP. From Visser [Visser, 2012]

1.2 Previous research

As part of the 'Knowledge for Climate' research program, Deltares has been conducting extensive research [Goes et al., 2009, de Louw et al., 2011, van Baaren et al., 2012] on the hydrogeological state of the Province of Zeeland. Van Meerten already has done research of artificial infiltration in creek ridges [van Meerten, 1986]. Research has been done on the fresh water - salt water distribution by modelling the groundwater for the entire province [van Baaren et al., 2012]. De Louw [de Louw et al., 2011] has done research on the evolution of rainwater lenses and De Louw and Oude Essink [Goes et al., 2009] have done studies on using geophysical measurements to measure fresh-salt interfaces at depths up to several meters.

Visser [Visser, 2012] has already done a modelling study on the properties of Sanderse and Louwerse. By making use of the density dependent groundwater flow code MOC-DENS3D [Oude Essink, 1999], Visser modelled the formation of the freshwater lens to the current situation. In addition,Visser modelled the effects of increased ditch level and artificial infiltration of fresh water on the freshwater lens. Results show significant (up to several meters) lowering of the fresh-salt interface, which indicates the possibility of storing excess freshwater in the creek ridge.

2. Research goals and approach

2.1 Research goals

In the pilot study, the evolution and continuous change of the freshwater lens is monitored after implementation of the level-controlled drainage system throughout several years. The freshwater lens will be monitored using a variety of measurements which are explained in the Methods section. Besides this, an adapted version of the model of Visser is used to model the evolution of the freshwater lens. The model makes use of the density dependent groundwater flow code SEAWAT [Guo and Langevin, 2002]. The current situation will be calibrated on the available measurements (groundwater levels, sample analysis etc.).

The calibrated model can then be used as a tool to model changes in the future. The following effects on the fresh-salt interface will be modelled:

1. Climate change as defined by the Royal Dutch Meteorological Instite (*KNMI*)
2. Detailed (daily, weekly) changes in precipitation and evaporation of several years (2011, 2012 and 2013)
3. Implementation of the level controlled drainage system on short time scales as well as long time scales

In addition, since the same model has been used with two different numerical groundwater codes, a comparison can be made based between MOCDENS3D and SEAWAT. The current situation of both models is used as a reference and the results will be compared in terms of accuracy, numerical dispersion and runtime. Further differences between the model by Visser and this model is the way the infiltration is modelled as is explained in the Model Description section.

2.2 Approach

A stepwise approach is taken to come up with the a calibrated model which can be used making long term and short term predictions on the evolution of the freshwater lens.

1. Model the current day situation from initial saline conditions. Calibrate the model to the field measurements.
2. Perform a sensitivity analysis to determine the sensitivity of model parameters
3. Model several years (2011, 2012, 2013) on a daily basis to determine the short term effects
4. Run scenarios in order to determine the effects of climate change and the implementation of the drainage system
5. Compare the results between the climate and infiltration scenarios

This study is of importance since this will give valuable insight in the evolution of the freshwater lens due to climate effects and implemented drainage. From this study, the farmers could decide on taking possible measures in the near future to prevent crop damage if needed.

3. Hydrogeological setting of the study area

3.1 Geological history of the province of Zeeland, the Netherlands

The geological history of Zeeland dates back several thousands years (Holecene period). The mainland in Zeeland consists of three geological distinctive formations: (1) Reclaimed tidal marshes consisting of peat and clay (0-2m under mean sea level), (2) sand dunes next to the shoreline (5-30m above mean sea level) and (3) ancient creeks filled with laminated sand and clay (0-2m above sea level) [Vos and van Heeringen, 1997]. The fresh-brackish-salt water interfaces are found to be quite shallow since the landmass in Zeeland is in all directions very close to the North Sea. Because of the increasing land subsidence of the peaty soil and rising sea level, freshwater availibility is decreasing and will continue to decrease in the coming decades. This puts a lot of stress on farmers which are largely dependent on fresh water in drier periods during the summer months.

3.2 The creek ridge system

The creek ridge stretches from south-west near Middelburg and Vlissingen all the way to the dune area near Domburg. The properties of Sanderse and Louwerse are exactly on the creek ridge north-west of Serooskerke. North-west of the property of Sanderse the creek ridge broadens in a fan shape until the dunes. The creekridge is bordered in the west by a road and in the east and north by a 2-3m deep brackish water ditch which cuts through the creek ridge. The ditch is draining saline water from depth up to the surface. The part of the creek ridge above the brackish ditch is still part of the natural creek ridge system, but it is not of interest to this study since this study focuses on enlarging the freshwater supply on the properties of Sanderse and Louwerse. For the remaining part of this paper, the combined properties of Sanderse and Louwerse will be named as the creek ridge. In the creek ridge itself, the soil mostly consists of sand up to 20 m below surface level (18.5 m NAP). The most eastern part of the creek ridge on the left bank of the brackish ditch is more clayey and already at much lesser elevation (0 m +NAP). On the left side of the road (the western part of the model), surface elevation is also much lower (0.5 m NAP). The soil is also very clayey with almost no changes in elevation. EM31 measurements by Visser [Visser, 2012] show that the depth to saline water is very close to surface level. Infiltration in this clayey soil is very difficult and slow. The part on the eastern bank of the brackish ditch is higher compared to the western part, but consists of peat instead of sand or clay. Due to the higher elevation and different soil type, the fresh-brackish-saline water interface is deeper here than in the west. Perpendicular to the brackish water ditch on the north side of the creek ridge and separated by a dike, a freshwater ditch is flowing to a weir where it is held.

3.2.1 Geological setting at the field study site

A cross section perpendicular over the creek ridge lets us divide the study site into 3 different zones: (A) West of the creek ridge, (B) the creek ridge and (C) East of the creek ridge. Elevation maps also show the distinctive height creek ridge. The top of the creek ridge is a 1.5 m above NAP while the lower areas west and east are at level with NAP. The model domain has been boxed in 1.1.4 and 3.2.2. The sandy creek deposits reach until depths of 20 m below mean sea level. The geological data has been used as a guideline for model input. The actual geological input was the same as was used in the model by Visser [Visser, 2012] and was provided by GeoTOP.

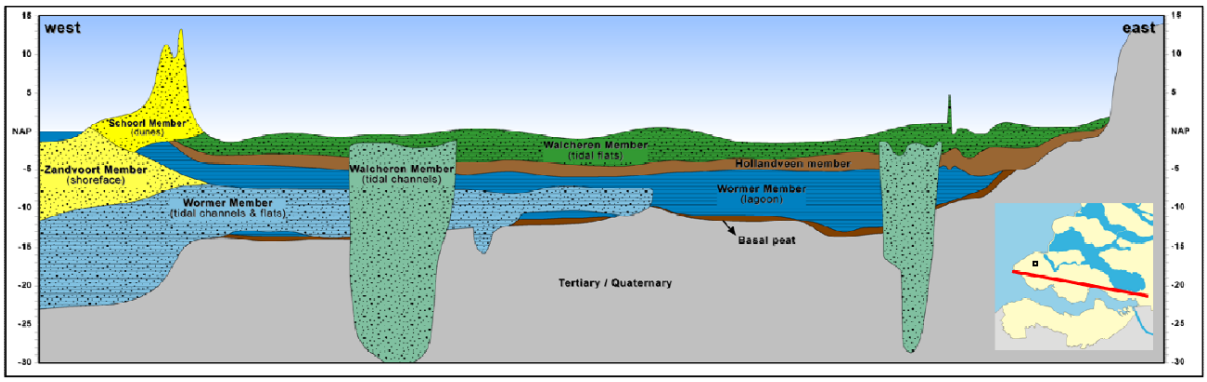

Figure 3.2.1: General geological setting of Walcheren

Zone	Depth (m -NAP)	Lithological unit
A	0 - 1	Duinkerke deposits (clays)
	1 - 2	Holland Peat
	2 - 9	Calais deposits (clay and sand)
	9 - 9.5	Basal Peat
	9.5 - 80	Pleistocene deposits (sands)
B	-1.5 - 0.5	Duinkerke deposits (clays)
	0.5 - 20	Duinkerke deposits (sand)
	20 - 80	Pleistocene deposits
C	-1.5 - 1	Duinkerke deposits (clays)
	1 - 2	Holland Peat
	2 - 10	Calais deposits
	10 - 80	Pleistocene deposits

Table 3.2.1: General lithology of the field site [van Betuw, 1952]

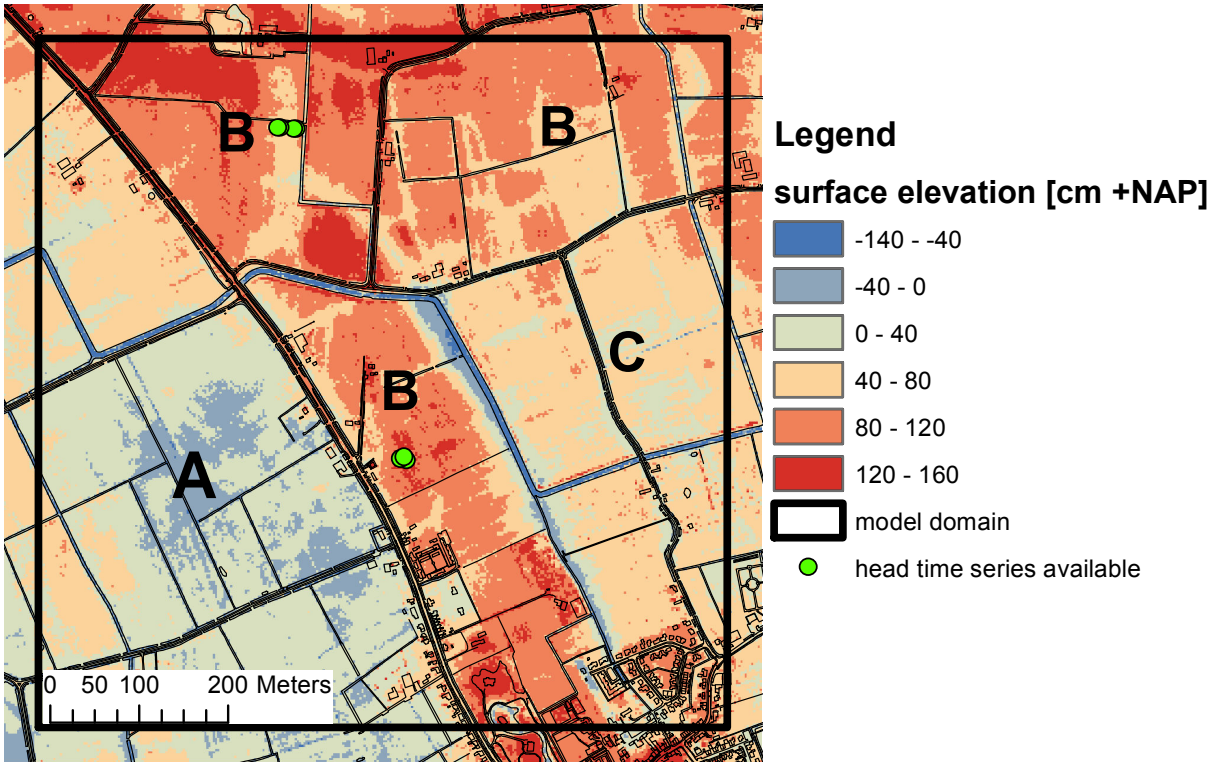

Figure 3.2.2: Surface elevation and model domain (black box). The areas with letters B are all part of the creek ridge, which are the highet areas. The creek ridge is cut off by a brackish water ditch on the northern border of the property of Sanderse. This cuts the property of Sanderse of from the northern part. The western part A is lowlying and almost no freshwater is present in the soil. The eastern C part is somewhat higher than area A, but it is not known what the thickness of the freshwater lens here is.

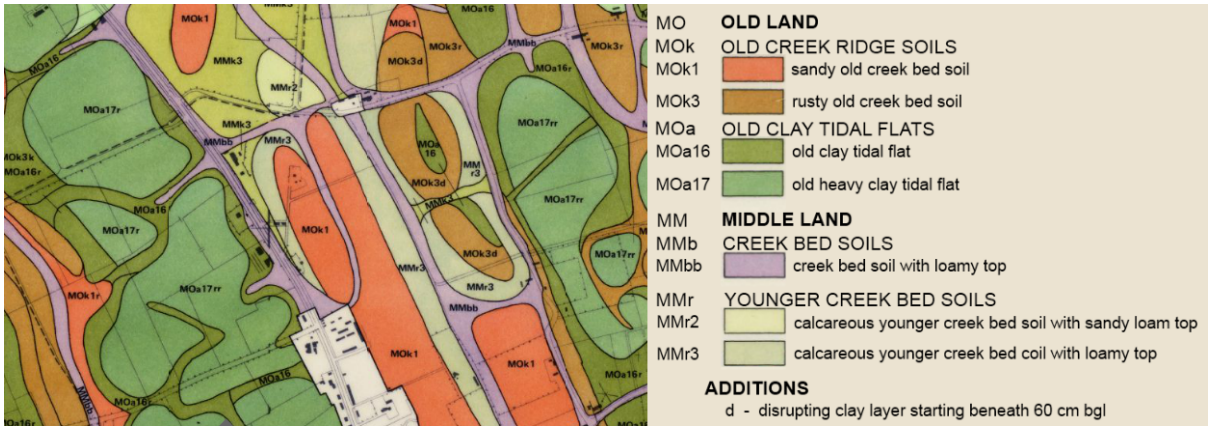

Figure 3.2.3: Soil map of the field site [van Betuw, 1952].The creek ridge predominantly consists of 'sandy old creek bed soil', but the eastern part of area B is a younger more calcareous bed with loamy top.

4. Theoretical Framework

4.1 Level controlled drainage

In January 2013 the level controlled drainage was contructed on the properties of Sanderse and Louwerse. From a collection box behind the weir, water is pumped in a pipe over the brackish water ditch into an inlet well. If the pump is switched on, water flows from the inlet through the route with the smallest resistance which is initially the main pipe, due to the large diameters. After these have been filled completely, the water flows through the drainage pipes which have smaller diameters and water in leaked through the pipes. From this moment on, water is effectively infiltrating in the subsurface. The pump is regulated automatically. If the water level in the inlet well is too high, the pump is shut off. Then the water level in the inlet well will drop. If the water level in the inlet well is too low for a certain amount of time, the pump will automatically be switch on again. By infiltrating the water, this will raise the groundwater level. To prevent the soil of becoming too wet and to prevent the groundwater of flowing to the ditches, the groundwater level can be regulated. The groundwater can be maintained in stages close to the ditch. If the water level in the creek ridge is to higher, then the level is dropped and water can flow to the ditch.

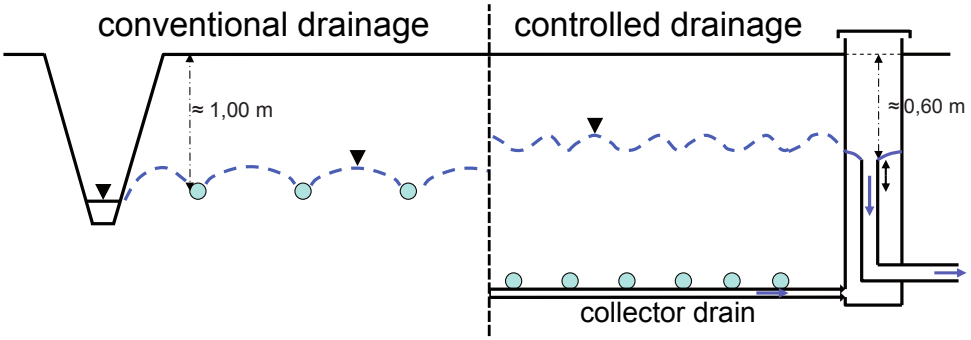

Figure 4.1.1: Schematic view of the level controlled drainage system and the differences with conventional drainage. The outflow level in the well on the righthand side is managable. If the groundwater level rises above the outlet level, water will be flow out of the aquifer and the level of the outlet height is maintained as groundwater level. Image after van Bakel et al. [van Bakel et al., 2008], received from Visser [Visser, 2012].

The implemented drainage system for the fields of Sanderse and Louwerse is depicted in figures 4.1.2 and 4.1.3 respectively. The grey dots show the wells where the level is controlled. The red line is the main transport drains. Water from the inlet point (grey dot in the upper left corner of figure 4.1.2 flows first through the main drain which has a diameter of 160 mm. It then ends in the well at the bottom of figure 4.1.2 where it connects to the blue main drain on the property of Louwerse. When both main drains the proterties have been filled, water will start flowing in the infiltration drains and seep into the soil.

If the groundwater level at any stage would get to high and the soil will become too wet for the likes of the farmers, the level can be regulated with the wells close to the ditch. They lower the outlet level in the control well and water will flow from the aquifer into the ditch.

Figure 4.1.2: Drainage system on the property of Sanderse. Red and cyan lines are main drains with diameters of 160 mm and 125 mm respectively. The green and yellow lines represent infiltration drains with drain distances (distance inbetween drains) of 7 and 6 m respectively.

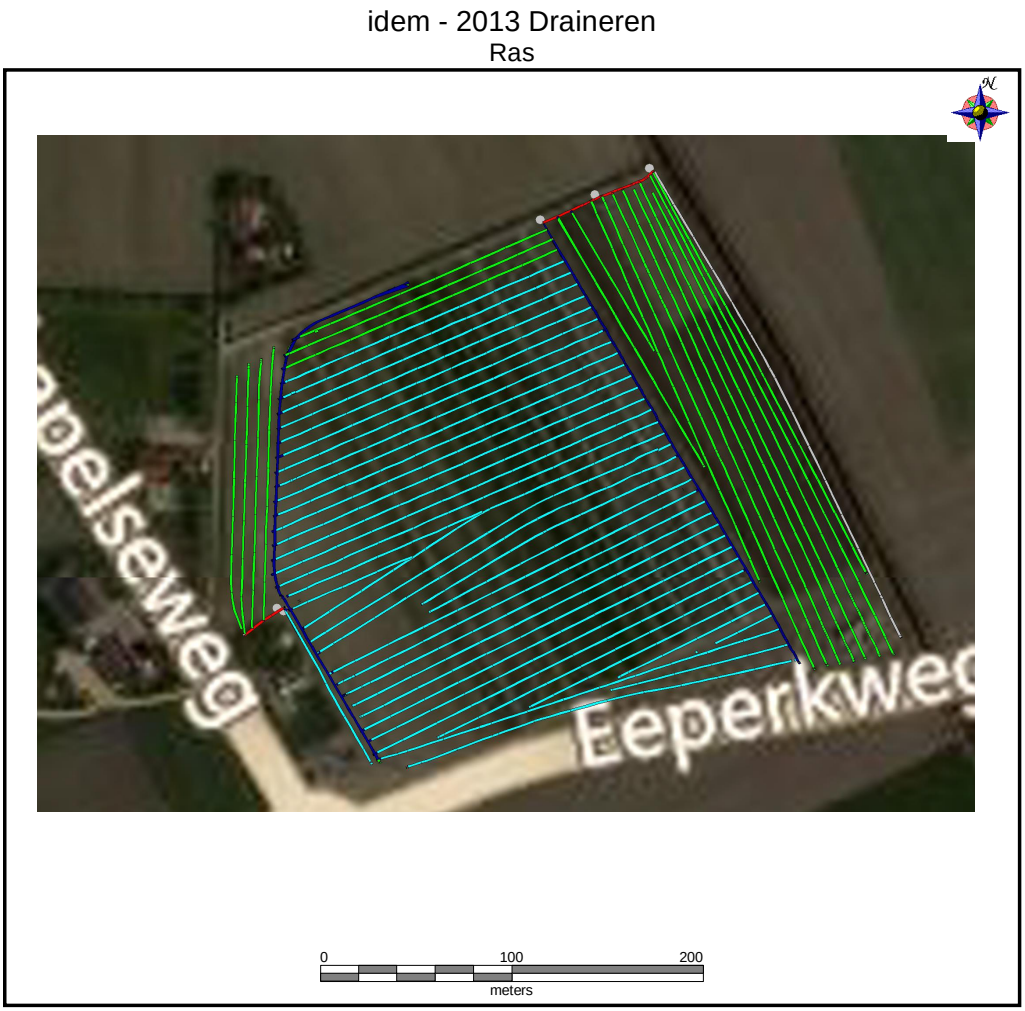

Figure 4.1.3: Drainage system on the property of Louwerse. Blue and red lines are main drains with diameters of 160 mm and 125 mm respectively. The cyan and green lines represent infiltration drains with drain distances (distance inbetween drains) of 7 and 6 m respectively.

4.2 Groundwater Flow

Flow of fluids through porous media was first extensively studied by Darcy [Fitts, 2002]. This was the first time flow of water through a porous medium (e.g. soil) could be quantified:

$$Q_s = -K_s A \frac{dh}{ds} \tag{4.2.1}$$

Here Q_s is the water flow [L^3 T^{-1}] in the s-direction, A [L^2] is the cross-sectional area perpendicular to s through which water flows, $\frac{dh}{ds}$ [-] is the head difference dh [L] over horizontal distance ds [L]. K_s [L T^{-1}] is the hydraulic conductivity of the porous medium. A is often ruled out in the equation by dividing the equation the equation through A. This results in the Darcy equation:

$$q_s = -K_s \frac{dh}{ds} \tag{4.2.2}$$

In this case q_s is the groundwater flux in the s-direction [LT^{-1}] and the other parameters are the same as in equation 1. In general, 3-dimensional (3D) flow is considered to flow in the plane of the landsurface (x- and y-direction) and perpendicular to the plane of the landsurface (z-direction):

$$q_x = -K_x \frac{dh}{dx},\ q_y = -K_y \frac{dh}{dy},\ q_z = -K_z \frac{dh}{dz} \tag{4.2.3}$$

4.3 Density dependent flow

Hydraulic conductivity K is not only a property of the soil type, but also of various other parameters [Fitts, 2002]:

$$K = \frac{\kappa \rho g}{\mu} \tag{4.3.1}$$

K is the hydraulic conductivity [LT^{-1}], κ is the intrinsic permeability of the soil [L^2], g is the gravitational acceleration and ρ and μ are the density [ML^{-3}] and dynamic viscosity [ML^{-1} T^{-1}] of the fluid respectively. In addition, often it is for hydrologists more convenient to measure hydraulic heads, which are applicable directly into the equations they use. Post et al. gave a definition for *equivalent freshwater head*, which is the head measured in a piezometer if all the water in the piezometer were to be freshwater:

$$h_f = \frac{P}{\rho_f g} + z \tag{4.3.2}$$

where h_f is the *equivalent freshwater head* [L], P is the fluid pressure [ML^{-2}], ρ_f is the density of freshwater, g is the gravitational acceleration and z is the elevation head.

Substituting equations (4.3.1) and (4.3.2) into equation (4.2.3) and assuming fresh water, the Darcy equations become the following

$$q_x = -\frac{\kappa\rho_f g}{\mu}\frac{d}{dx}\left(\frac{P}{\rho_f g} + z\right) = -\frac{\kappa}{\mu}\frac{dP}{dx}, \tag{4.3.3}$$

$$q_y = -\frac{\kappa\rho_f g}{\mu}\frac{d}{dy}\left(\frac{P}{\rho_f g} + z\right) = -\frac{\kappa}{\mu}\frac{dP}{dy}, \tag{4.3.4}$$

$$q_z = -\frac{\kappa\rho_f g}{\mu}\frac{d}{dz}\left(\frac{P}{\rho_f g} + z\right) = -\frac{\kappa}{\mu}\left(\frac{dP}{dz} + \rho_f g\right) \tag{4.3.5}$$

In systems where water density differences with depth are negligible, the effect of freshwater head cen be neglected and point water head will suffice. In the case of *hydrostatic equilibrium* ($q_z = 0$) a graph of head as a function of depth $h(z)$ will result in a straight line, since $\frac{dh}{dz} = 0$. However, this is not the case for systems where fresh water lies on top of saline waters and density differences cannot be neglected. To calculate here whether there is hydrostatic equilibrium, the point water heads should be converted into freshwater heads [Post, Kooi and Simmons, 2007]:

$$h_{f,i} = \frac{\rho_i}{\rho_f}h_i - \frac{\rho_i - \rho_f}{\rho_f}z_i \tag{4.3.6}$$

Calculating the freshwater head at depth i and calculating the freshwater head at depth $z = 0$ will yield in a head gradient. If this gradient is also 0, there is hydrostatic equilibrium.

4.4 Solute Transport

The transport of solutes in porous media is another important aspect of groundwater flow. Several processes like advection, dispersion, absorption, adsorbtion, chemical reactions and degradation all affect the concentration of a solute in groundwater. The total equation of solute transport including all terms above is [Zheng and Bennet, 1995]:

$$\frac{\partial(\theta C^k)}{\partial t} = \frac{\partial}{\partial x}\left(\theta D\frac{\partial C^k}{\partial x}\right) - \frac{\partial}{\partial x}\left(\theta q_i C^k\right) + q_s C_s^k + \sum R_n \tag{4.4.1}$$

C^k is the concentration of solute k [ML^{-3}], θ is porosity of the porous medium [-], D_{ij} is the *hydrodynamic dispersion coefficient*, q_i is the Darcy velocity [LT^{-1}], q_s is the Darcy flux [LT^{-1}] entering/leaving the system from sources or sinks, C_s^k is the concentration of solute k [ML^{-3}] entering/leaving the system from sources or sinks and R_n are the fluxes of reaction and decay of solute k.

Since chloride is a conservative solute (non-absorbing, reactive, decaying solute), we neglect the last two terms in the equation (nummer) and we devide by θ:

$$\frac{\partial^2 C^{Cl}}{\partial t^2} = D_x\frac{\partial^2 C^{Cl}}{\partial x^2} - v_x\frac{\partial C^{Cl}}{\partial x} \tag{4.4.2}$$

In this equation $D_x \frac{\partial^2 C^{Cl}}{\partial x^2}$ is called the *dispersion* term and $v_x \frac{\partial C^{Cl}}{\partial x}$ is the *advective* term. Advection is the transport of solute due to the flow of the host fluid. Hydrodynamic dispersion is the sum of *mechanical dispersion* and molecular diffusion. The latter is the natural flow of solutes to flow from areas of high concentration to low concentration. Mechanical dispersion is the changes in concentration caused by the effect that the solute cannot flow in a straight line, but it has to flow in a tortuous path around the grains in the soil.

The 1D-mechanical dispersion flux is a form of Fick's first law [Fitts, 2002]:

$$F_x = -\theta D x \frac{\partial C}{\partial x} \tag{4.4.3}$$

D_x is the dispersion coefficient parameter which is the sum of the molecular diffusion term and the mechanical dispersion term [Fitts, 2002]:

$$D_x = \alpha_x |\overline{v}| + T_x D_{mol} \tag{4.4.4}$$

In this equation α_x is the dispersivity in the x-direction [L], $|\overline{v}|$ is the absolute value of the average flow velocity [LT^{-1}], T_x is the tortuosity in the x-direction [-] and D_{mol} is the molecular diffusion coefficient [L^2T^{-1}]. In almost all cases dispersivity is many orders of magnitude higher than the molecular dispersion coefficient and it can be neglected.

Dispersivity in the flow direction is called longitudinal dispersivity , α_L while dispersivity perpendicular to the flow direction is called transversal dispersivity, α_T. As a rule of thumb, this approximate relation is used:

$$\alpha_T \approx 0.1 \cdot \alpha_L \tag{4.4.5}$$

4.5 Ghyben - Herzberg principle

Badon Ghyben and Herzberg [**?**] were among the first hydrologists who investigated the evolution of freshwater lenses on top of saltwater, originally formed on islands.

The Ghyben-Herzberg principle is one of the most widely used methods for calculating the thicknesses of freshwater lenses and although it is not the most accurate method and it has it's limitations, the principle still holds and forms the basis for several more complicated mathematical solutions. The Badon Ghyden-Herzberg principle states that freshwater lenses above saline groundwater can be formed due to buoyancy forces of the salt water. Fresh water, which has a lower density than salt water are assumed to be nearly immiscible. When precipitation (freshwater) falls on an island in an ocean where the groundwater is completely saline, a freshwater lens will form. The thickness of the lens is dependent on the point where the pressure of the salt water at that point equals the pressure of the freshwater column above it. This is mathematically defined as:

$$\rho_s H g = \rho_f H g + \rho_f h g \tag{4.5.1}$$

The term on the left hand side is the total pressure of a column of salt water with density ρ_s and depth H. The term on the right hand side is the density of the column of freshwater above the salt water, where H is the depth to the salt water relative to mean

sea level, h is the groundwater level above mean sea level and so $H + h$ equals the total length of the freshwater column. Rearranging the formula gives:

$$h = \frac{\rho_s - \rho_f}{\rho_f} H \tag{4.5.2}$$

In equation (4.5.2) $\frac{\rho_s - \rho_f}{\rho_f}$ is called the buoyancy term, which is a linear factor α which relates the groundwater level on the island to the thickness of the freshwater lens only related on the relative density of water. For the remainder of this research freshwater has a density of 1000 kg/m^3 and salt water has a density of 1025 kg/m^3. Filling in these values will yield into the relation that for every 1 m of groundwater h, we have 40 m of freshwater below it. This is in reality a severe overestimation. However, the principle still holds and will form the basis of the idea of level controlled drainage. Increasing the groundwater level will result in a lowering of the depth to the fresh-salt interface.

4.6 Modelling Groundwater Flow

4.6.1 SEAWAT vs. MOCDENS3D

In simple 2-dimensional (2D) groundwater problems with no density differences in water, homogeneous geology and constant parameters, simple groundwater equations will suffice for most problems. However, when it comes to dealing with complex 3D groundwater problems with heterogeneous soil and parameters which are not constant with depth or time, one has to model the problem using one of the many available groundwater codes which are currently available. Numerical groundwater flow codes consist often of various modules which deal with different parts of the total equation(s). The model used in this study uses the numerical code SEAWAT [Guo and Langevin, 2002], developed by the United States Geological Survey (USGS). The same model has been run using another numerical code MOCDENS3D [Oude Essink, 1999], which is the MOC3D code by Konikow [Konikow and Goode, 1996] adapted for density dependent flow.

Model runs are devided into *stress periods* which are further divided in *timesteps*. Stress periods are certain periods of length t where boundary heads and flow fluxes are constant. For example, recharge fluxes can be defined for specific stress periods or levels in river cells are set for certain stress periods. Dividing the stress period into smaller timesteps is more accurate, since the flow equation is solved for every timestep and therefore the calculated hydraulic head field is updated every timestep. If the length of the stress period is not to long, deviding the stress period into smaller timesteps is unnecessary since groundwater flow is an overall slow process. However, if stress periods have lengths of several months, the devision is needed and the flow field has to be updated several times to avoid accuracy errors. One can also choose to model with more timesteps for the sake of accuracy or if more output times are desired.

The numerical codes SEAWAT and MOCDENS3D consist of three parts: (1) flow, (2) the solute transport and (3) density dependancy. For the flow part, both codes use the MODFLOW program. MODFLOW is a block-centered, numerical computer code which is able to solve groundwater flow equations in three-dimensions using a finite-difference

solver method. The program is continuously updated with additional modules (packages) which extend the possibilities of the program greatly. A disadvantage is that MODFLOW alone does not deal with density dependancy and therefore it is not suitable by itself for problems where density differences are significant (brines, sea water intrusion etc.).

The biggest differences in the codes are found in the solute transport part and the coupling of the flow and transport equation. In SEAWAT, the solute tranport part is solved by the MT3DMS module [Zheng and Wang, 1998] which is the mass transport code MT3D with the addition of the possibility of modelling multiple species simultanuously. The variable density part is implemented by the addition of a Variable Density Flow module (VDF). The density field (density values for all cells) are calculated by a defined equation of state which relates the concentration of solute to the density. For salt-fresh water problems it is convenient to choose the chloride concentration as the reference concentration, since it is by far the most contributing element to salinity and therefore density. The equation of state in the VDF module is:

$$\rho(C) = \rho_f(1 + \alpha\frac{C}{C_s}) \tag{4.6.1}$$

The density value at a certain concentration of chloride $\rho(C)$ is related to the chloride concentration by a reference density (of fresh water) ρ_f, a reference concentration C_s which is the concentration of chloride in sea water (= 18630 mg/L) and the buoyancy term α.

The coupling between MODFLOW and MT3DMS can be both explicit and implicit and are both explained in detail in the SEAWAT user guide [Guo and Langevin, 2002]. The procedure is as follows: (1) The flow equation is solved by MODFLOW with the head distribution, this yields the advective fluxes (in 3 directions) for the transport equation. (2) The transport equation is solved with the calculated advective fluxes of step 1. This gives the concentration values. (3) The newly obtained concentration values are in turn used to update the density field. (4) The density field updates the head distribution in all cells, which can be used in the next flow timestep. In every MODFLOW timestep, the transport equation will be solved multiple times. The *transport timestep* is the time for which the transport equation is solved and is calculated from spatial discretization parameters, dispersion parameters and flow velocities. If smaller transport timesteps are calculated then the transport equation has to be solved more times per MODFLOW timestep. Usually this would not be a problem, but very small transport timesteps could lead to undesirably long and unpractical run times. The longer run times are caused by the coupling of the flow and solute transport equations. In SEAWAT the flow equation is solved for every transport timestep, while for MOCDENS3D it is solved for every MODFLOW timestep only.

The solute tranport equation can be solved using several different solver methods: (1) the Method-Of-Characteristics, *MOC*, (2) the Modified-Method-Of-Characteristics, *MMOC* (3) the Hybrid-Method-Of-Characteristics, *HMOC*, (4) the finite-difference method and (5) the Total-Variation-Diminishing (TVD) solver. Which solver to use is dependent on the problem and the desired amount of accuracy in the results. Also time

constraints can be a factor since some solver methods [(5)] can have very long run times. Detailed explanations of these solvers are given in the SEAWAT User's guide [Langevin and Guo, 2002].

MOCDENS3D on the other hand uses the MOC3D module [Konikow and Goode, 1996] adapted for density dependent flow for the solute transport and density dependency part. The same MOC module as in MT3DMS is used, however apart from the MOC solver no other solvers are available. The MOC module splits advective and dispersion terms of transport and solves them independently. Advective transport is solved by the particle tracking method, while the dispersion term is solved by a finite difference method.

In short, the differences are given here:

Table 4.6.1: Differences between SEAWAT and MOCDENS3D code

	SEAWAT	MOCDENS3D
base code	MODFLOW + MT3DMS	MODFLOW + MOC3D
head input	Salt water head	Fresh water head
Solvers	MOC, HMOC, MMOC, FD, TVD	MOC
Concentration of RIV, GHB and WEL cells	In SSM package	In RIV, GHB, WEL package
Multispecies modelling	Yes	No

5. Methods

5.1 Overview of measurements

For monitoring the freshwater lens over the year various measurements have been used. All measurements are listed in table 5.1.1 and locations in on the field site are either given in fig. 5.1.1 for the Continuous Vertical Electrical Sounding measurements or fig. 5.2.1 for all other measurement locations.

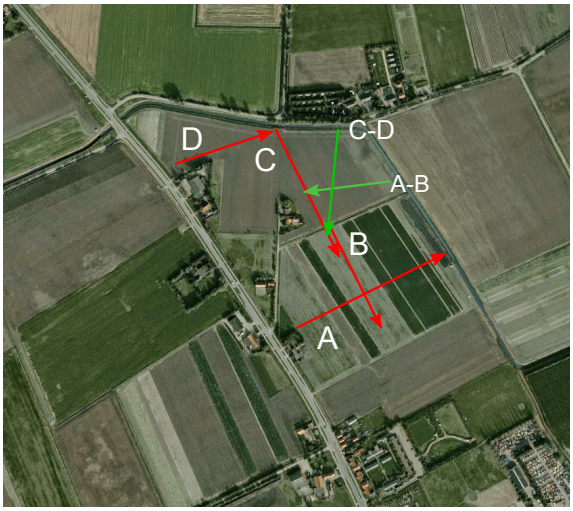

Figure 5.1.1: Locations of CVES profiles measured in October 2012. An enlargement is also included in the Appendix.

	Amount	Location in fig 5.2.1	Goal
Monitoring wells	12	all	Measuring groundwater levels, groundwater sampling
Groundwater samples	20	I, II and III	Concentration of solutes in groundwater, inlet water and ditch water
Continuous Vertical Electrical Sounding	6	fig. 5.1.1	Obtain transects on fresh-salt interface depth
Slimflex	6	I, II,III,D,E,F	depth profile on lithology/fresh-salt interface
Subsurface Monitoring Device	1	II	continuous measuring of fresh-salt interface

Table 5.1.1: Overview of measurent techniques, amount, locations and purpose of the measurement

5.2 Monitoring wells

Monitoring wells were installed on several locations in the area. The names of the monitoring wells and locations are given in table 5.2.1. Various measurements have been done in these monitoring wells with the purpose of calibrating the model en to monitor the freshwater infiltration experiment. The locations of the monitoring wells are given in 5.2.1. The borehole analysis results are given in the appendix. For the remainder of this thesis, monitoring wells are mentioned by their given name in table 5.2.1.

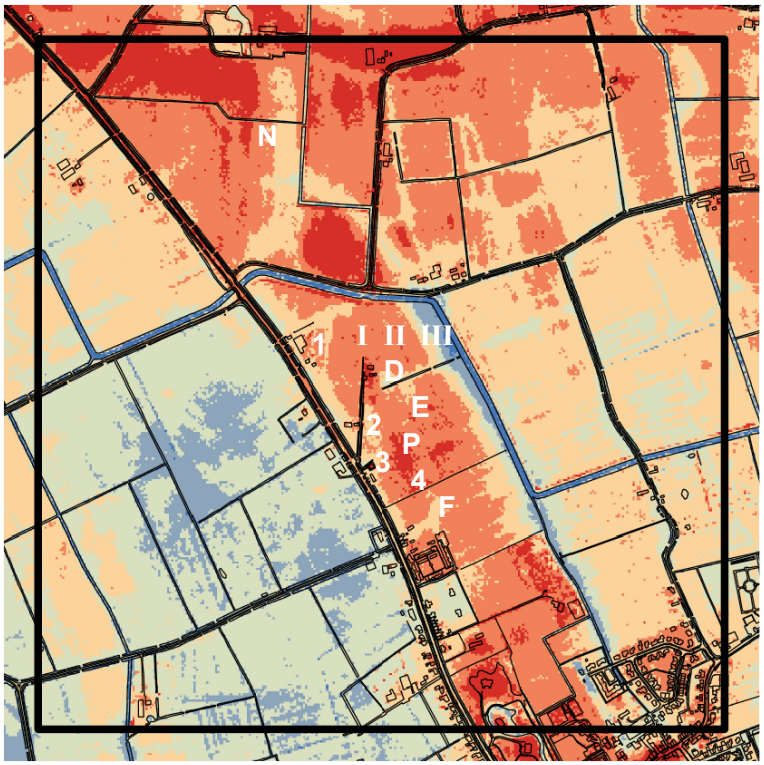

Figure 5.2.1: Locations of the monitoring wells (white numbers) within the model domain (edge). The locations are coded conform the code given to the monitoring well in table 5.2.1/ At locations I (Minifilters I), III (Minifilters III) and E (Slimflex E) the borehole analysis is measured in the same borehole as the Slimflex measurements. At location II, Minifilters II is situated. The borehole analysis is done in the borehole of the Subsurface Monitoring Device which is located 5 m west of II. An enlargement is also included in the Appendix.

At the locations of Minifilters I, Minifilters II and Minifilters III, 7 monitoring wells are placed with filters at different depth. This was done to be able to sample groundwater and measure electrical conductivity at different depth. The deepest well at each location 4, 5 or 6 is the one where the Slimflex measurements have been done (Slimflex A, B and C respectively. In all 7 wells, electrical conductivity has been measured and groundwater samples were taken in all wells of locations 4 and 5. At every measurement location (except North), groundwater levels have been measured.

Table 5.2.1: Names of monitoring wells and measurents taken in these monitoring wells.(+)-signs indicates the measurements has been done in these monitoring wells, while (-)-signs indicate that these measurements have not be done in the monitoring wells. The location numbers are given in figure 5.2.1.

Code	Monitoring well	Diver data	Groundwater sampling	Electrical conductivity measure-ments	Slimflex measure-ments
1	Phreatic 1	+	-	-	-
2	Phreatic 2	+	-	-	-
3	Phreatic 3	+	-	-	-
I	Slimflex A/ Minifilters I	+	+	+	+
II	Slimflex B/ Minifilters II/ SMD	+	+	+	+
III	Slimflex C/ Minifilters III	+	+	+	+
D	Slimflex D	+	-	-	+
E	Slimflex E	+	-	-	+
F	Slimflex F	+	-	-	+
P	Pumping well	+	-	-	-
4	Phreatic 4	+	-	-	-
N	North	+	-	-	-

5.3 Groundwater sampling, EC-measurements and sample analysis

Groundwater samples were taken at the end of May 2013 and analyzed in the lab in order to find the chemical composition of the (1) infiltration (ditch) water, (2) the shallow (brackish) groundwater, (3) the groundwater on the fresh salt interface and (4) the saline groundwater. The groundwater was sampled from monitoring wells using a pump charged by a battery. The samples were collected in 100 ml bottles to which 60 umol of 1 M nitric acid has been added in advance to sampling. Acidifying the sample to pH = 2 gives better preservation of the elements needed for analysis. The samples were collected from the 7 monitoring wells at locations I and II, in the inlet pipe of the infitration system and the brackish water ditch (both are located directly north of location I (figure 5.2.1). Bicarbonate was measured in the field using a double titration method by a titrator. pH was measured by the same device with a pH electrode.

On the day of sampling (May 30th, 2013), weather conditions were not good and the fields were very wet due much precipitation of the days before. Therefore, location III was not accesible and only one sample was taken in the deepest well of location III (Slimflex C). Samples were transported to the lab on the same day and immediately stored in the fridge at 5 degree Celsius until the samples were analyzed.

Total element concentrations (for example $[Cl_{total}]$) were measured by an *Inductively Coupled Plasma Optical Emission Spectrometer*, ICP-OES. The results of the analysis are total concentrations of all the different (trace) elements. The advantage of ICP-OES is that the analysis is very accurate since even trace elements can be measured. A disadvantage of this analysis is that the results do not make distinctions for different species of certain elements. For example, the total amount of sodium $[Na_{total}]$ is given and not the different species.

Electrical conductivity is measured in monitoring wells several times over a timespan of several months (period April 2013 - May 2013). EC was measured in situ with an EC meter which has been calibrated in advance. Groundwater was pumped up at Minifilters I, Minifilters II and Minifilters III of containing 7 monitoring wells each which have minifilters at different depths. In this way, EC could be measured at the same location for different depths. Water was pumped up using a pump and water was stored in a beaker with outflow to collect a sample of uniform EC. The water was pumped up using a rubber tube which had a measuring scale attached to it in order to accurately (error = 10 cm) measure the depth at which the water pumped. The electrode of the EC meter was injected in the beaker in order to measure EC. To include the error in EC, two values of EC were obtained. The first value was the first value the EC meter gave, while the second value is the value at which was assumed equilibrium had been reached. The EC-meter automatically corrects the measured EC-values for EC at a temperature of 25 degree Celsius.

TNO [Goes et al., 2009] has come up with an empirical relationship which relates electrical conductivity of the water to chloride concentration. The only other dependent value in the fomula is the bicarbonate concentration:

$$[Cl^-] = (\frac{EC_{w,20} - 0.122[HCO_3^-]}{0.44096})^{\frac{1}{0.9446}} \tag{5.3.1}$$

$[Cl^-]$ is the chloride concentration in mg/L, $EC_{w,20}$ is the electrical conductivity of groundwater at 20 C in mS/m, $[HCO_3^-]$ is the bicarbonate concentration in mg/L. This conversion will be used often in this paper to convert the measured and modelled EC and $[Cl^-]$ into each other.

For the continuation of this thesis, the Stuyfzand classification [Stuyfzand, 1986] for groundwater based on chloride concentration is used. This classification will be used predominantly in coloured contour plots of concentration and to classify the type of groundwater.

Table 5.3.1: Classification of groundwater type based on chloride concentration (in mg/L)

Type of groundwater	Range of Chloride concentrations (mg/L)
fresh	<150
fresh-brackish	150 - 300
brackish	300 - 1000
brackish-saline	1000 - 10000
saline	10000 - 20000
hypersaline or brine	>20000

5.4 Continuous Vertical Electrical Sounding

Continuous Vertical Electrical Sounding (CVES) is a geophysical method for determining apparent soil resistivity (combined effect of both soil resistivity and water resistivity) by measuring the electrical potential difference. A series of metal electrodes are placed into the soil. The device sends an electrical current through the two active electrodes and the electrical potential difference is measured (in Volts). Various setups for measurement are known (Wenner, Schlumberger [Pauw, 2012]), but the used method in this study is the Wenner method. In the Wenner method all the electrodes are equally spaced apart. The measure differences in Volts are monitored in a data processor and stored in 2D-arrays. The 2D-arrays contain apparent resistivities that can be converted to formation resistivities using an inversion code. The results are plotted in 2D-cross sections of transects. Since the method does not calculate groundwater resisitivity but bulk resistivity, comparing the results with the electrical conductivity measurements is not so precise as would have been if one would have obtained groundwater resistivity. However, combined with the other measurements, the CVES transects give good approximations of the depth to the fresh-brackish-saline interface.

For comparison with other measurements the resistivity values [Ωm] can be converted to conductivity values [mS/cm] by:

$$C_w[mS/cm] = 10\frac{1}{R_w}[\Omega m] \tag{5.4.1}$$

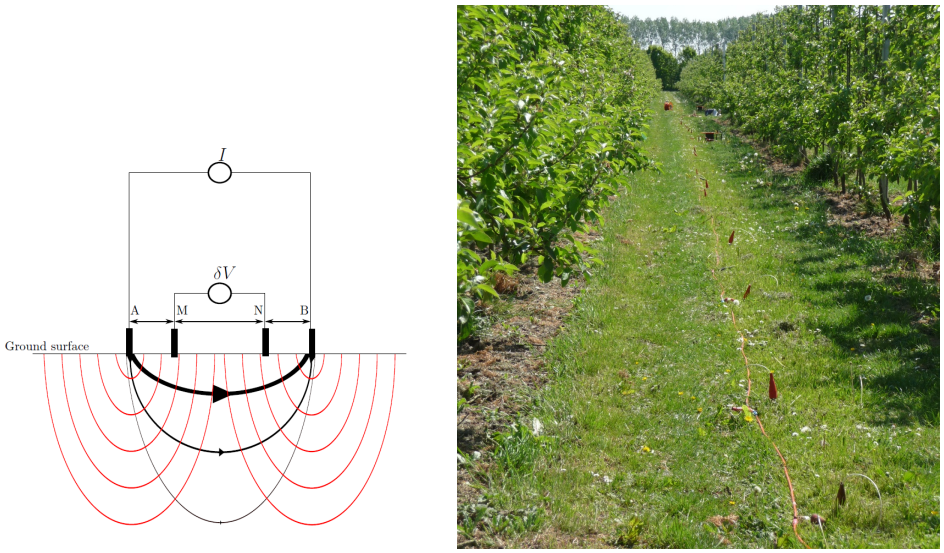

Figure 5.4.1: Schematic setup and picture of a CVES measurement. The red lines are equipotential lines and current flow lines are the black lines (which are perpendicular to the equipotential lines). The battery I delivers the power. The potential difference δV between the active electrodes is recorded by the data processor. Picture from [Pauw, 2012].

5.5 SlimFlex

SlimFlex is a geophysical, electomagnetic measurement method which measures the soil resistivity in Ohm m , ρ_s. Water resistivity ρ_w can be deduced from ρ_s by the formation factor of the soil [Goes et al., 2009].

$$\frac{\rho_s}{\rho_w} = F \tag{5.5.1}$$

Formation factor is dependent on several parameters (lithology, porosity, tortuosity), so in order to make determine the formation factor in a column borehole logs are examined for changes in lithology. Borehole logs are taken in 4 Slimflex tubes (Slimflex A, Slimflex B, Slimflex C and Slimflex D). They can be found in the Appendix. The classification for formation factors which is used is given here [Goes et al., 2009]:

Table 5.5.1: Formation factors for certain lithological units [Goes et al., 2009]. Asteriks indicate apparent or approximate formation factors.

Lithology	Formation factor (F)
Gravel with sand	7
Coarse sand with gravel	6
Coarse sand	5
Intermediate sand	4
Slightly clayish sand	3
Intermediate clayish sand	2.5*
Heavily clayish sand	2*
Clay	1-3*
Peat	1

5.6 Subsurface Monitoring Device

The company ImaGeau has installed a Subsurface Monitoring Device (SMD), which constantly measures electrical resistivity of the pore fluid around the borehole. Since this system is fully automatic, the data is constantly being distributed. The device is a vertical cilinder probe with electrode with variable spacing. Finer spacing (1 electrode/10 cm) is used on the area of interest; the fresh-salt interface and coarser spacing is used in the shallower and deeper groundwater. The SMD measures apparent soil resisitivity R_0 to a distance of 1 meter away from the device and every minute. Temperature and pressure sensors in the electrodes continuously measure temperature and pressure, since several parameters like conductivity are dependent on temperature. The measured electrical resistivity is then converted to electrical conductivity of the pore fluid:

$$\frac{1}{R_0} = C_0 = \frac{C_w}{F} S_w^2 + C_S \tag{5.6.1}$$

Here R_0 is the electrical resistivity of the bulk soil, C_0 is the conductivity of the bulk soil, C_w is the electrical conductivity of the pore fluid,S_w is the water saturation, C_S is the conductivity of the soil and F is the formation factor of the soil, ϕ is the porosity of the soil and m a constant:

$$F = \phi^{-m} \tag{5.6.2}$$

The SMD is calibrated on the lithology of the soil. This includes the parameters porosity, electrical conductivity of the pore fluid and the conductivity of the soil. All parameters are obtained by borehole analysis done by Fugro. The results are given in the appendix.

The SMD is located approximately 5 m west of Minifilters II (fig. 5.2.1). The measurements are sent by satellite connection and are accesible by Deltares and ImaGeau. The SMD was installed on December 9th 2012 and has been running continuously.

6. Measurement Results

6.1 CVES results

Throughout the year 2011, 4 CVES transects were measured (A, B, C and D). In addition, 2 more CVES transects were measured in October 2012 which are called A-B and C-D. All transect locations are given in 5.1.1. Red arrows are the transects measured in 2011, while green arrows are measured in Oktober 2012. The arrows give the directions of measuring.

The scales in the resistivity plots are an approximation of the fresh-brackish-salt interface. The blue part has apparent resisitivity values of 25 Ωm and higher. The red part starts where apparent resistivities are 5 Ωm or lower. There are contours with values of 20, 15 and 10 Ωm inbetween. Apparent resistivities can be converted in groundwater EC by using formulas 5.4.1 and 5.5.1. The only dependent parameter is the formation factor F (section 5.5). Choosing the correct formation factor is very important for geophysical methods [Jacobs, 2013]. The corresponding values of the contour values are given in figure 6.1.1. Extrapolating the lines to $\rho_s = 0$, will yield in a groundwater EC which goes to infinity. From figure (6.1.1) it is can be concluded that choosing a correct formation factor is important and that is has implications on defining the fresh-brackish interface and the brackish-saline interface. For example, if we define freshwater to have a maximum EC of 1 μS/cm, then the fresh-brackish interface for $F = 1$ is at $\rho_s = 10$ Ωm, while for F = 6, it is found at an even higher value than $\rho_s = 25$ Ωm. Moreover, since the lithology of the soil is heterogeneous, it is important to use different values of F for different depths. Therefore, for the sake of simplicity, it is chosen to assume freshwater to have a minimum value of 25 Ωm for ρ_s and salt water to have a maximum value of 5 Ωm for ρ_s. This will coincide with the blue and red contourlines of the CVES plots.

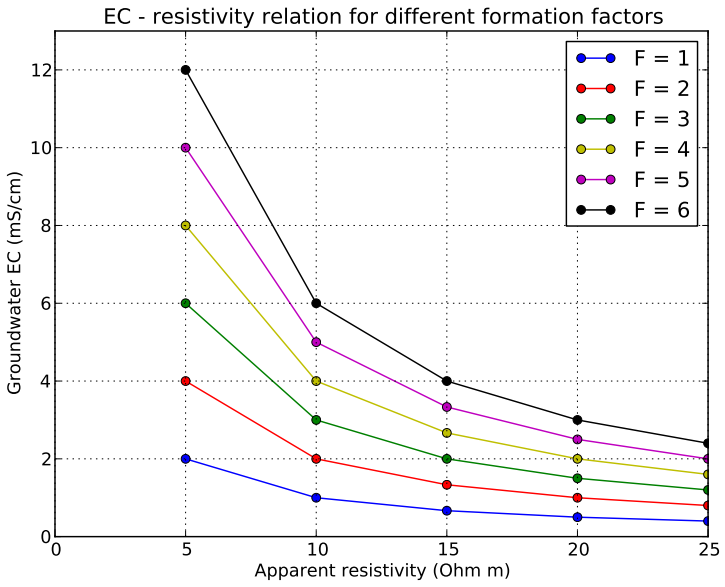

Figure 6.1.1: Corresponding EC_w values to ρ_s values, calculated for different formation factors.

Transect A

This transect is made perpendicular to the creek ridge and should give a good indication of the maximum thickness of the freshwater lens. The maximum depth of the freshwater lens is measured here to a maximum depth of 13.5 m -NAP in the middle of the creek ridge. The mixing zone has a thickness of around 3 meters. On the right side of the transect you can see the influence of the brackish water ditch, since the mixing zone is very sharp there. It would seem that salt water is flowing upwards, which could explain the sharper interface.

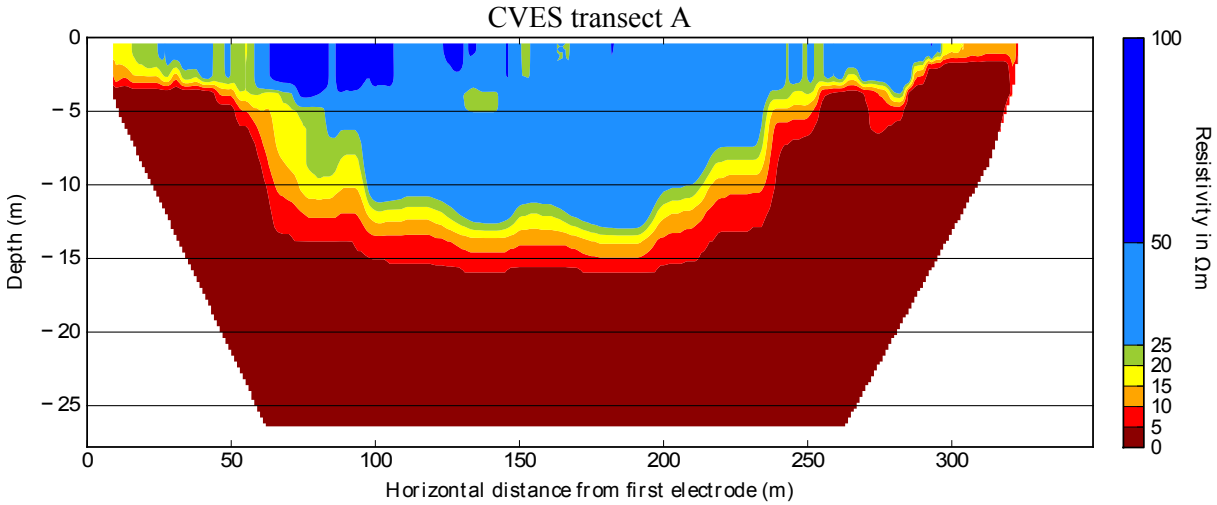

Figure 6.1.2: CVES transect of line A as given in 5.1.1.

Transect B

Transect B runs from the middle of the creek ridge near the small ditch between the properties of Louwerse and Sanderse to the south end of the field of Louwerse, where another small ditch is located. The transect gives results as expected. We see upconing on the edges of the transect due to the ditches there and a maximum depth of the freshwater lens of 13.5 m -NAP, which is the same as measured in Transect A.

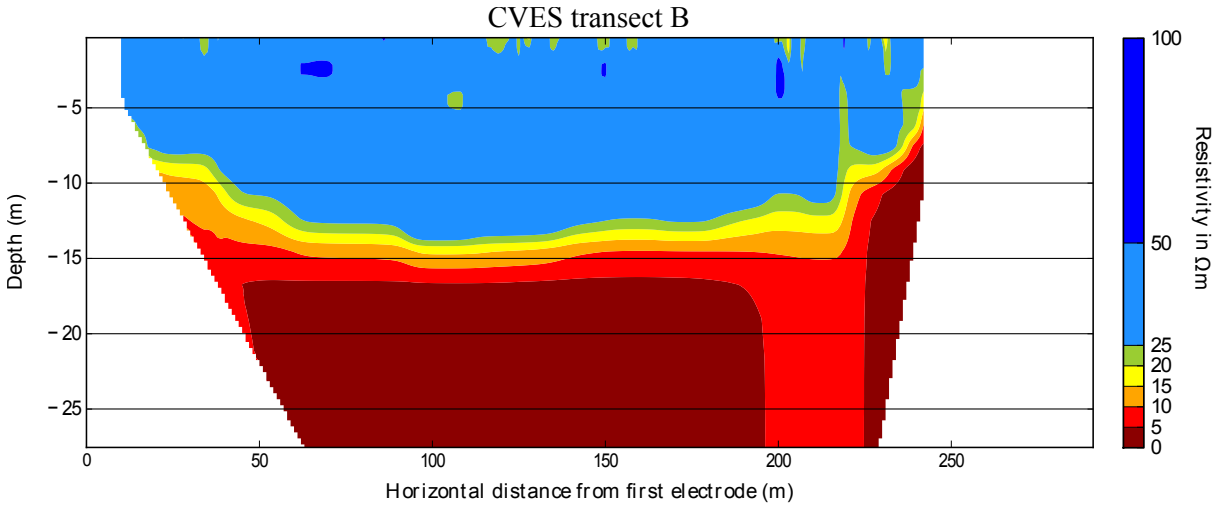

Figure 6.1.3: CVES transect of line B as given in 5.1.1.

Transect C

Transect C is taken across the north end of the property of Sanderse, near the brackish

water ditch over the creek ridge. The peak at $x = 50$ m is an error caused by an electrical cable which distorts the electrical currents of the measurement. Depths to the mixing zone on the property of Sanderse are around 10 m -NAP. The transect runs in between Minfilters I and Minifilters II at around $x = 130$ m. The upconing at $x = 200$ is caused by the small ditch in between the properties of Sanderse and Louwerse.

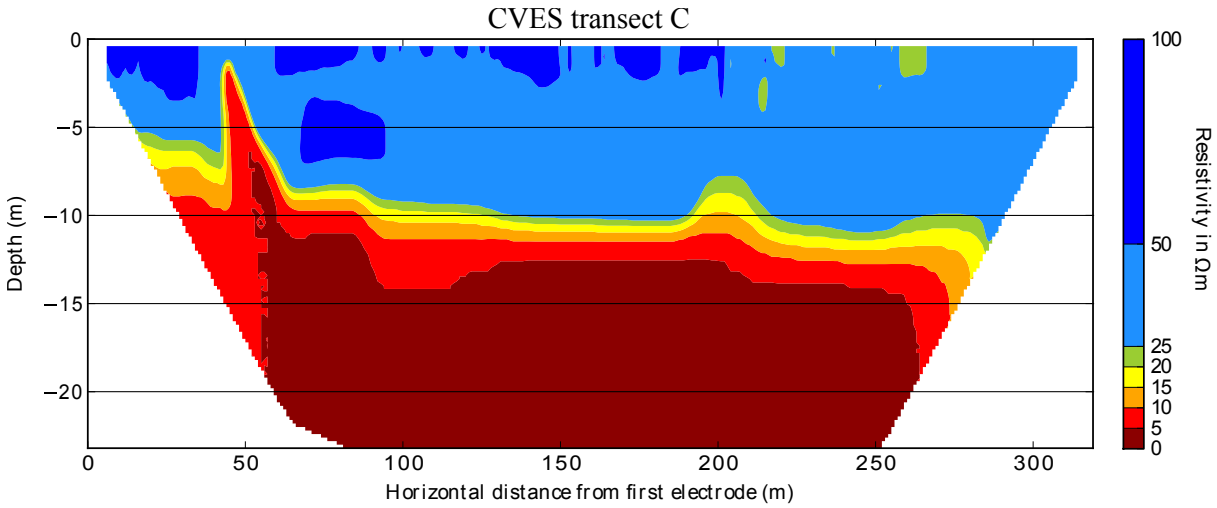

Figure 6.1.4: CVES transect of line C as given in 5.1.1.

Transect D

Transect D is taken not on the properties of Louwerse nor Sanderse, but is still located on the creek ridge just to the west of the property of Sanderse and infiltration is expected have an effect on this area as well. The transect runs from the road in the north-east direction to the northwestern point of the property of Sanderse. There is no freshwater lens close to the road. The freshwater lens is present at $x = 40m$ where the lens is very shallow with a thickness of just a few meters. The maximum thickness is located at $x = 120m$ where the lens is 9 meters thick.

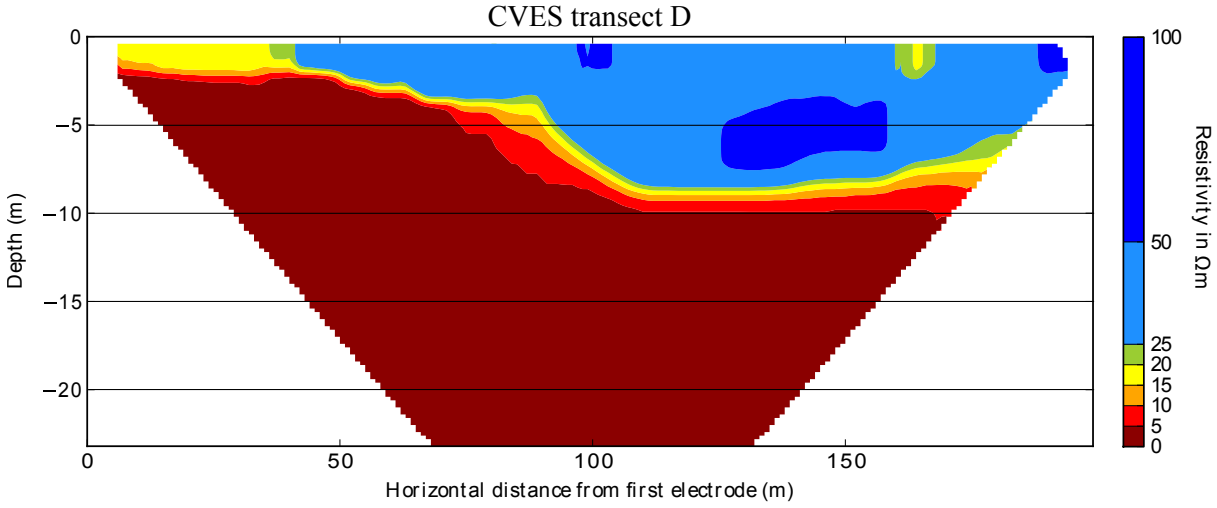

Figure 6.1.5: CVES transect of line D as given in 5.1.1.

Transect A-B

The transect is taken starting very close to the brackish water ditch in the east. The transect goes along all three monitoring wells with Slimflex A/Minfilters I, Slimflex B/Minfilters II and Slimflex C/Minfilters III. Minifilters III is located almost at the beginning of the transect at $x = 40$ m, Minifilters II is located around $x = 100$ m and Minifilters III is located at the end at $x = 140$ m. The transect is not directly on the line of the three monitoring wells, but it will be a good approximation. According to these results, the depths to saline water are $x = 40$ m, $x = 100$ m and $x = 140$ m, 2 m, 8 m and 14 m respectively. Mixing zone thicknesses are 0.5 m, 2 m and 2 m respectively.

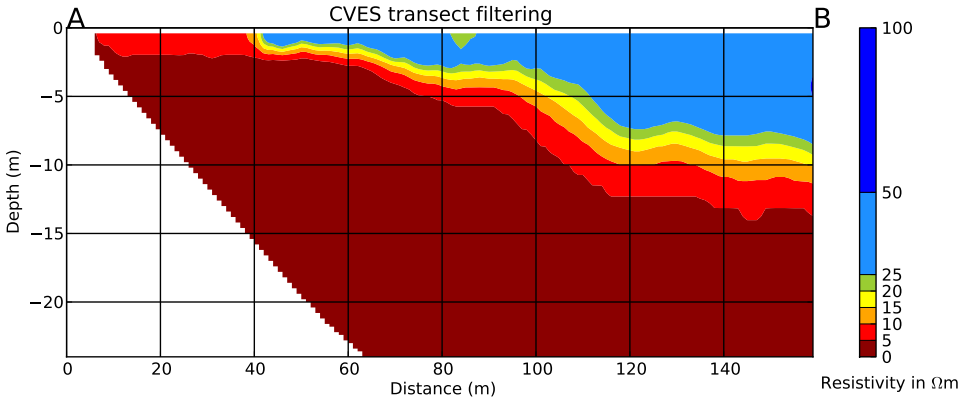

Figure 6.1.6: CVES transect of line A-B as given in 5.1.1. At $x = 100$ the monitoring well with Slimflex A/Minifilters I is situated.

Transect C-D

CVES transect was taken in October 2012. The transect runs from the brackish water ditch in the north up to the tertiary ditch in the middle of the creek ridge. The fresh-water lens is very shallow very close to the ditch where fresh water is only found in the top few meters. Along the transect at a distance of around 80 m the monitoring well with Slimflex B/Minifilters II is situated. According to these measurements the depth to the mixing zone is 8 m - NAP, while the thickness of the mixing zone is quite high (5 m).

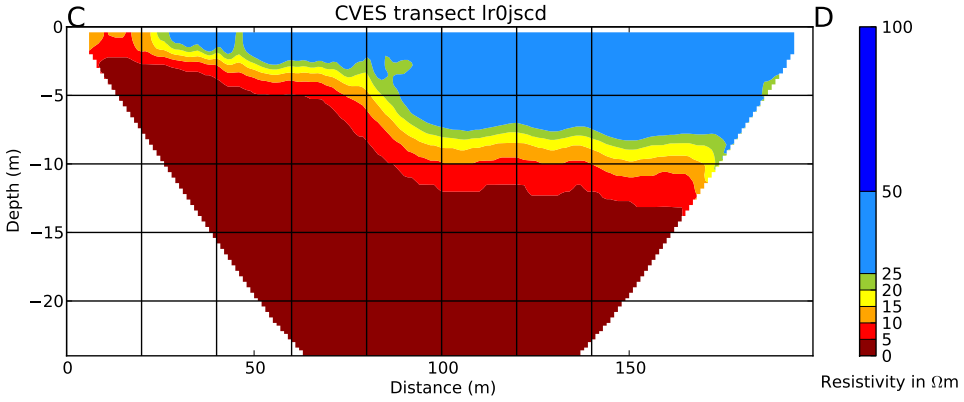

Figure 6.1.7: CVES transect of line C-D as given in 5.1.1.

6.2 EC-measurements results

The measured EC values of pumped up groundwater in the monitoring wells Minifilters I, Minifilters II and Minifilters III are plotted with depth in figure 6.2.1. Since the first set of measurements are done before infiltration started (26-04-2013) and the second set of measurements were done after several days of infiltration (30-05-2013), it would theoritically have been possible to see some effect of freshening on the fresh-salt interface. The measured electrical conductivities measured in monitoring wells Minifilters I and Minifilters II on 30-05-2013 are both lower than the electrical conductivities measured on 26-04-2013. For Minifilters I changes in EC are measurable at depths starting -11 m, -14 m and -15.5 m. At a depth of -19 m, no change in EC is observed. In Minifilters II changes in EC are observed at depths -9 m, -10 m, -11 m and -11.5 m.

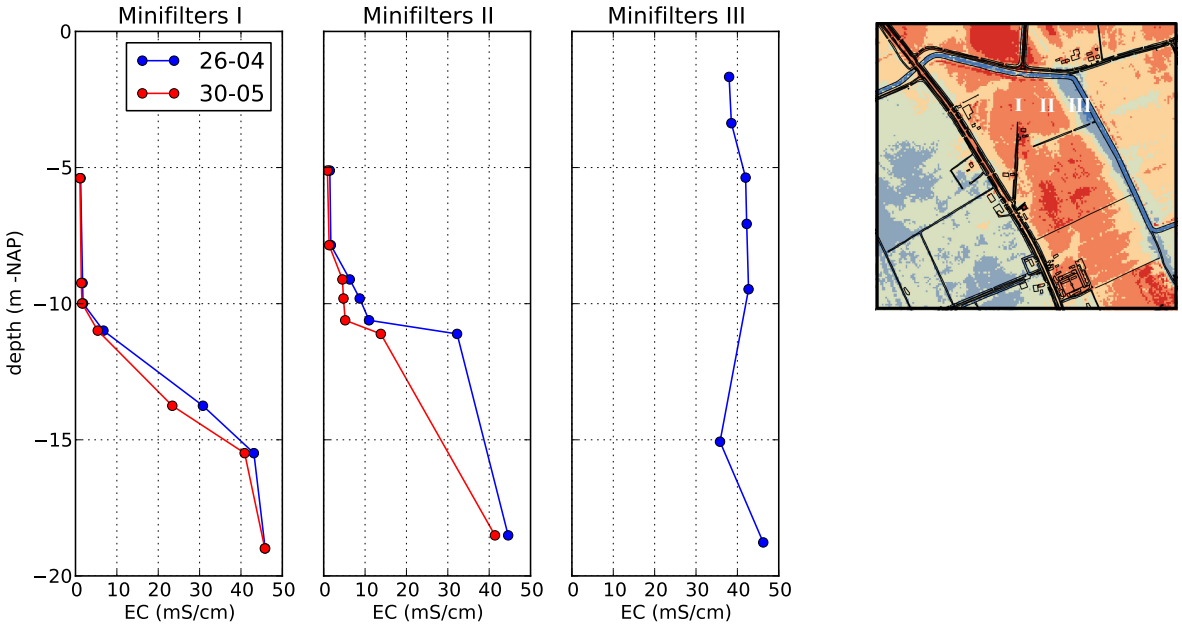

Figure 6.2.1: Measured electrical conductivity values of pumped of groundwater in monitoring wells Minifilters I, Minifilters II and Minifilters III. The blue and red lines represent the values measured on 26-04-2013 and 30-05-2013 (before and during infiltration) respectively.

6.3 Slimflex

In figure 6.3.1 the measurements by the Slimflex device have been plotted. The bulk EC represents the combined effect of the soil and the groundwater. The measured EC_{bulk} is significantly lower than the direct EC measurements on the groundwater have showed. A conversion would be possible if an overall formation factor is known, which could be obtained from borehole logs. Then the same approach could be used as was used for the CVES measurements. However, since the soil is very heterogeneous and very small clay layers alternate with sand layers, the EC_w plots would show large fluctuations. It was

therefore chosen to plot just the bulk EC, since although it does not show the correct values, the fresh-brackish saline interface can still be obtained from these graphs since the trend for the EC_w and EC_{bulk} graphs are the same.

The trends in Slimflex A and B are similar to the EC measurements in Minifilters I and II, which are respectively the same monitoring wells. The fresh-brackish-salt water interface starts at a depth of 10 m in Minifilters I and around 9 m in Minifilters II. Slimflex C is taken in the same well as Minifilters III, but not much can be said here since the soil is very clayey here. Slimflex D shows a shallow fresh-brackish-saline interface of around 6 m depth. This is explanable since Slimflex D is very close to the small ditch seperating the properties of Sanderse and Louwerse. Slimflex E and F show deeper interfaces at 11 m and 13 m respectively.

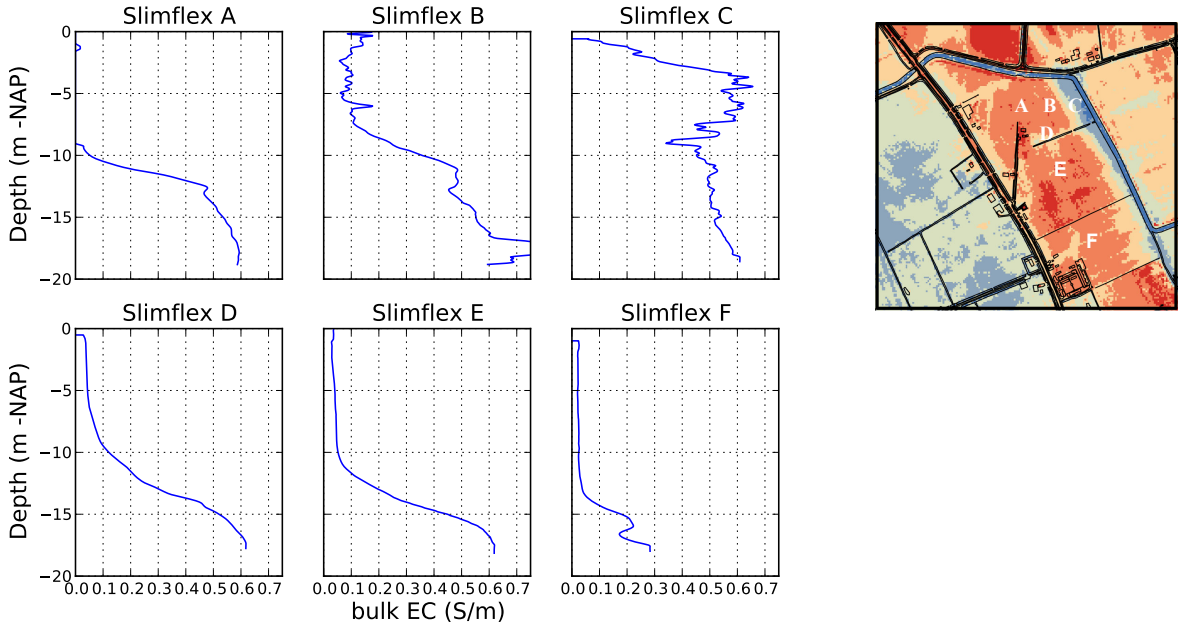

Figure 6.3.1: Profiles made by the Slimflex device. The plots do not give the electrical conductivity of the groundwater EC_s, but rather the bulk (soil + water) electrical hydraulic conductivity. Bulk EC and EC_w are related by the formation factor.

6.4 Groundwater sample analysis

The results of the chemical analysis fom the groundwater samples are given in table 6.4.1. The >- sign indicates an approximate value. During the analysis the sample has not been diluted. If the sample is not diluted, the ICP-OES wiil not give very accurate results when concentrations are over the maximum concentration limit ($\approx$ 300 mg/L). In this way samples from large depths had results out of the measurent range. The error of these values is at least 10 %, but can be much larger.

To check the influence of the error equation (5.3.1) was used to calculate the chloride concentration from the measured EC values and bicarbonate concentration. Since bicar-

bonate and EC were not measured with ICP-OES, the obtained value for the chloride concentration by calculation is independent of the measured chloride concentration. The results show that for shallow depth, the [Cl] measured by ICP-OES is very close to the calculated value. For larger depths, the calculated and measured values start to deviate slightly, with the calculated values showing larger concentrations. Since the fit between the measured and calculated values is quite good, it was assumed that in general the measured values are a good indication of the chloride concentration in the groundwater and they could be used as proxy for model calibration.

Table 6.4.1: Results of the chemical analysis of the groundwater samples taken in the monitoring wells on 30-05-2013. [Cl] is given in mg/kg which is equal to mg/L for freshwater, but not for saline water. Due to magnitude of the error in the results, the conversion to mg/L for saline waters is left out.

Monitoring well	depth (m + NAP)	[Cl] (mg/kg))	$[HCO_3^-]$ (mg/L)
Minifilters I well 6	-5.39	24	604
Minifilters I well 5	-9.24	77	599
Minifilters I well 4	-9.99	113	652
Minifilters I well 3	-10.99	>1376	773
Minifilters I well 2	-13.74	>8169	1120
Minifilters I well 1	-15.49	>13566	1437
Slimflex A	-18.99	>15198	973
Minifilters II well 6	-5.11	44	399
Minifilters II well 5	-7.86	107	512
Minifilters II well 4	-9.11	>969	678
Minifilters II well 3	-9.81	>1122	670
Minifilters II well 2	-10.61	>1290	616
Minifilters II well 1	-11.11	>4993	987
Slimflex B	-18.61	>13794	900
Inlet	-	70	
Saline water ditch	-	>342	

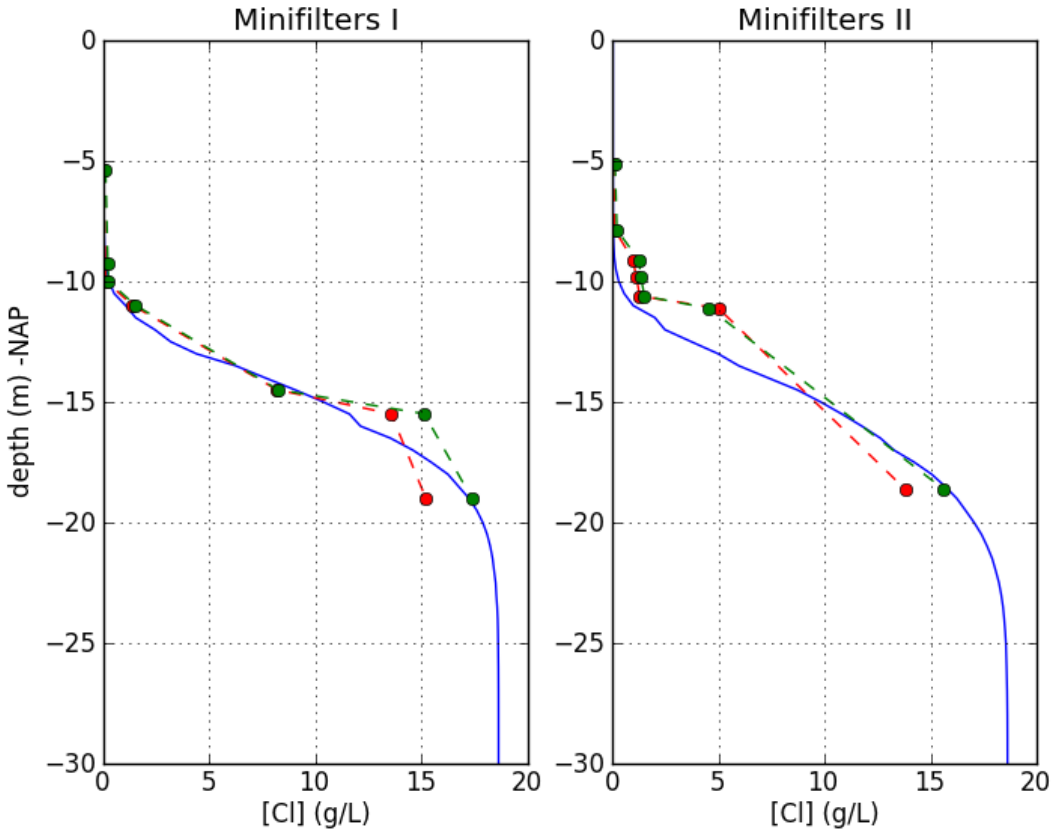

Figure 6.4.1: Depth profiles of the modelled and measured chloride concentration (g/L). The blue graph gives the modelled chloride concentration at Minifilters I and Minifilters II. The red dots represent the results of the groundwater sample analysis by ICP-OES and the green dots represent the calculated chloride concentrations from the electrical conductivity and bicarbonate values from table 6.4.1 using formula 5.3.1

6.5 Subsurface monitoring device

Data obtained from imaGeau was used as a comparison to the modelled [Cl] and EC measurements. The obtained data included apparent resisitivities and electrical conductivities. EC in (mS/cm) was plotted as depth profiles in 6.4.1 for 26-04-2013 and 30-05-2013. Since the Subsurface monitoring device is very close to Slimflex A and Minifilters I, the measured electrical conductivities at these days are a good approximation. For shallower depth up to 10 m -NAP, the EC is constant and very low. EC starts to rise from a depth of 10 m -NAP very steeply until a depth of 12 m -NAP, where the EC is constant again for 2 meters. Then at a depth of 14 m -NAP until a value of 43 mS/cm around 16 m - NAP. This would indicate that the thickness of the fresh-brackish-salt interface is at least 6 m thick. The resolution in the area of 8 m -NAP until 15 m -NAP is very high (1 electrode per 10 cm), but not high enough to accurately determine the part of the graph at depth 11 m -NAP. The largest change in EC with depth ,$\frac{dEC}{dz}$, is observed here. $\frac{dEC}{dz}$ becomes smaller then. This could be the effect of mixing between the infiltrating fresh water and the saline seepage water form depth. EC-measurements are almost all

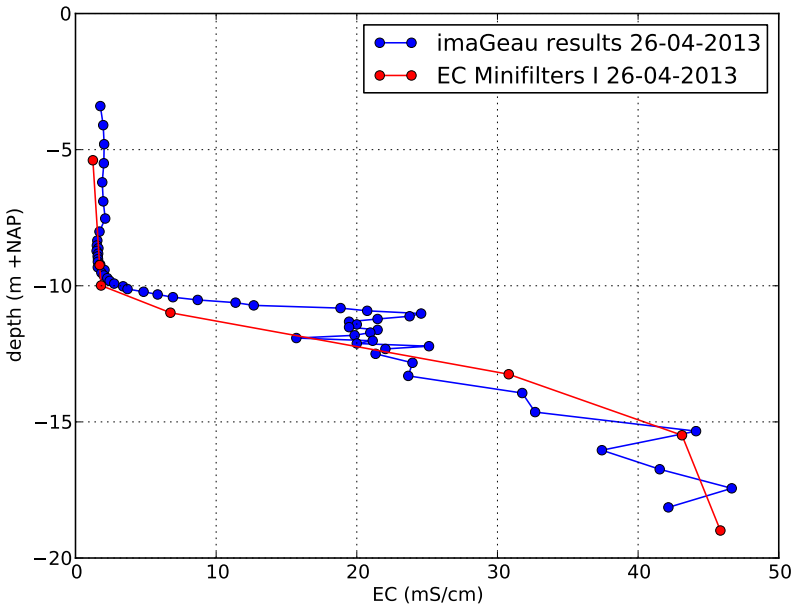

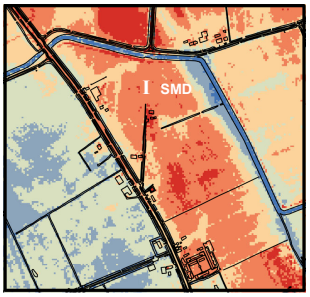

Figure 6.5.1: Depth profile of subsurface monitoring device (SMD) and EC measurements on 26th of April 2013

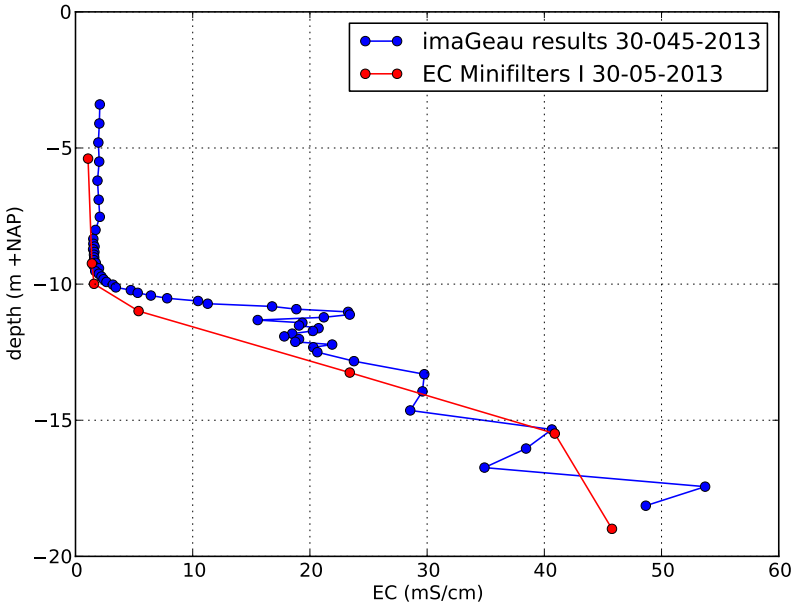

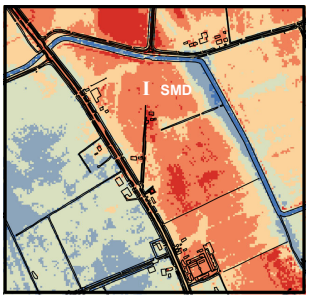

Figure 6.5.2: Depth profile of subsurface monitoring device (SMD) and EC measurements on 30th of May 2013

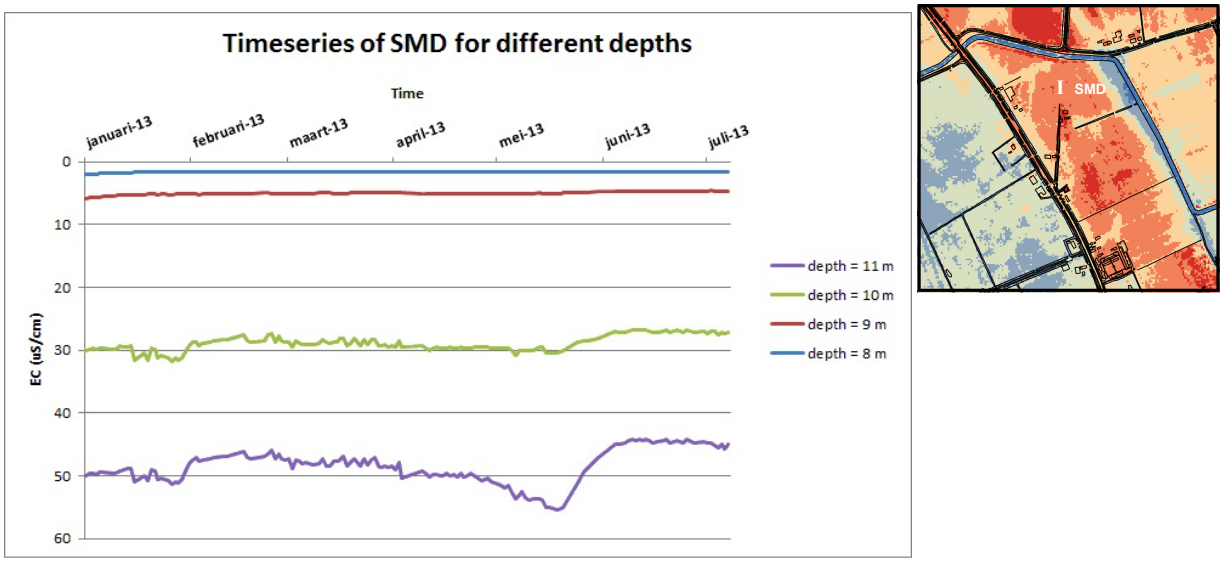

Figure 6.5.3: Timeseries of the EC (uS/cm) measured by the SMD at depths of 8 m, 9 m, 10 m and 11 m.

very close to the value measured by the SMD except for the point at depth 11.5 m -NAP where there is an offset with the SMD results.

Also timeseries have been made of various depths over time. In figure 6.5.3 timeseries are for 4 depths (8 m, 9 m , 10 m and 11 m) for the period of January 2013 until July 2013 are plotted. At depths 10 and 11 m there is little variation throughout the year. The jump in mid-May coincides with the start of the infiltration, which started on the 21st of May and went on until the 6th of June. Groundwater EC at depth 10 m and 11 m stay lower after infiltration has stopped.On shallower levels, less variation in EC is observed. Infiltration on short timescales is indeed measurable with the SMD.

6.6 Quality assessment of measurements

In order to look at the relative accuracy of the measurements and to give a qualitive impressions on how useful the different measurements are, all the measurements are compared for one location. The results for the SMD, CVES, Slimflex A, EC-measurements and groundwater samples are all converted to groundwater EC ($\mu S/cm$) and plotted for the location of Minifilter I. Only the SMD results are not directly measured at that location but approximately 50 m to the east.

As was explained in section (6.1), the conversion of bulk resistivity to groundwater EC is difficult because it is mostly determined by the formation factor (figure 6.1.1). In figure 6.6.1 the Slimflex results and CVES results are plotted with a formation factor of 6. This is the highest value of the formation factor for a sandy soil (table 5.5.1). Even with this high value, the CVES and Slimflex measurements still do no match with the other measurements. Lowering the formation will only lower the EC values even more. The CVES and Slimflex measurements are therefore the most inaccurate measurements . The SMD, EC and sample analysis results on the other hand seem to complement each other. A qualitive analysis given in table 6.6.1 .

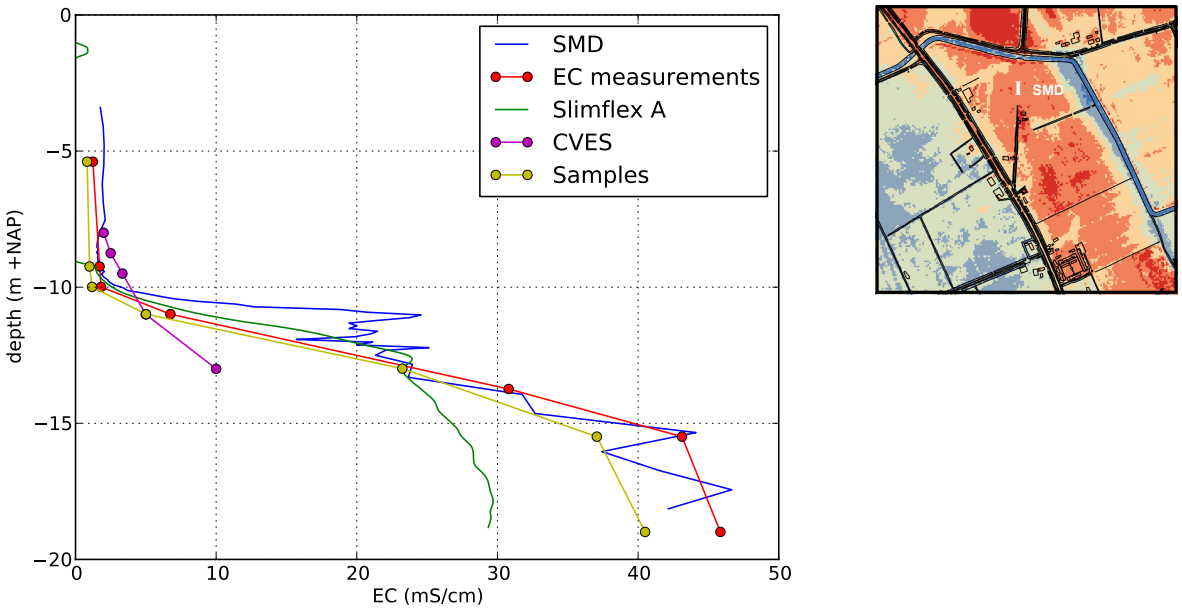

Figure 6.6.1: Comparison of 5 types of measurements at the location of Minifilters I. (1) The SMD measurements are retrieved from Imageau. (2) The EC-measurements are from table 4.1. (3) The Slimflex bulk conductivities are converted in groundwater conductivities using formulas 5.4.1 and 5.5.1 and using a formation factor (F) of 6. (4) The CVES values are taken from the contour plot of transect A-B (figure 6.1.6). The threshold values of soil resistivity (Ω m) are converted in groundwater conductivities (μ S/cm) by the means of formulas 5.4.1 and 5.5.1 and using a formation factor of 6. (5) The values of the chloride concentration are converted to groundwater EC by the means of formula 5.3.1 and the bicarbonate values in table 4.1.

Table 6.6.1: Qualitive analysis of the different measurement techniques. The measurement techniques are qualified in terms of accuracy (+, +/- or -). In the last column the explanation for the qualification is given.

Measurement	Accuracy	Explanation
SMD	+	Accurate measurement due to high resolution measuring and useful due to continuous measuring. Disadvantage is it is expensive and only measures at one location.
EC	+	Accurate and fast measurement.Direct measurements on groundwater EC with no conversion needed. Could be done often (once per month) for further monitoring.
Slimflex	+/-	Although the conversion of soil resistivity to groundwater EC is difficult, the shape of the depth profile can still be used as an indication on the thickness of the mixing zone.
CVES	-	Conversion of soil resistivity to groundwater EC is difficult. It is advised to use CVES measurements only as an approximate value for the size of the freshwater lens.
Sample analysis	+	Measuring chloride with ICP-OES is very accurate if analysis is done correctly. The results have been checked by converting the values to EC and they lie close to the EC measurements. Therefore, they are usable in this research.

7. Model description

7.1 Model setup

The geohydrological model used in this study is a density-dependent groundwater flow model, with coupled solute transport and adsorption processes. The code which has been used is SEAWAT, a combination of MODFLOW (groundwater flow) and MT3DMS (solute transport) adapted for density dependent flow. The basis of the model is the model built by Visser [Visser, 2012] which used the MOCDENS3D code. The reasons for switching to SEAWAT were that (1) SEAWAT is capable of modeling solute transport as well as density-dependent flow and (2) it would be possible to look at the same model with two different codes. From this it was expected the differences between the two codes would be visible. The layout of the model is given in the following table:

Table 7.1.1: model setup

Parameter	Symbol	unit	value
Number of rows	N_{row}	-	160
Number of columns	N_{col}	-	160
Number of layers	N_{lay}	-	80
Length of cells along rows	delc	m	10
Length of cells along columns	delr	m	10
Layer thickness	dz	m	(variable) 0.5 - 5
Model domain	-	m^2	1600 x1600
Stress period length	-	years	0.5
Number of time steps per stress period	t_{step}	-	6
Porosity	θ	-	0.35
Longitudinal dispersivity	α_L	m	0.1
Transversal dispersivity	α_T	m	0.01
Molecular Diffusion coefficient	D_{mol}	mol^{-1}	$8.64 \cdot 10^{-5}$

7.2 Boundary conditions

Boundary conditions were mostly the same as in the model used by Visser [Visser, 2012]. The top of the model is defined as the highest point of the creek ridge which is 1.5 m above NAP. Areas where the surface elevation is lower than 1.5 m above NAP have inactive layers at the top of their row/column. Since the top cells have thicknesses of 0.5 m, in practice the top 1 - 4 cells are inactive. The bottom of the model is taken at 87 m +NAP where there is a confining layer ($K_v = 2.5 \cdot 10^{-4}$). Because of the low vertical hydraulic conductivity value, the confining layer can be considered as a no-flow boundary.

The boundaries of the model are chosen 500 m away from the creek ridge. Several options for the head at the boundaries were available. A constant head boundary would not be a suitable option since heads in summer and winter differ significantly (+- 0.3 m). Therefore, a General-Head-Boundary was used. The General-Head-Boundary condition

does not give a certain constant flux to the cell but make it dependent on the difference between head of the GHB-cell with an adjacent cell with coordinates (i, j, k).

$$F = C(h_{ghb}^{i,j,k} - h^{i,j,k}) \tag{7.2.1}$$

To determine the fresh-brackish-saline interface, the chloride concentration [Cl] is modeled as a species. The salinity of sea water (S is the measure of the total mass in grams of solids dissolved per kg of seawater [Emerson and Hedges, 2008] is largely determined by chloride since chloride and sodium account for the vast majority in seawater. In freshwater this is different and other ions (bicarbonate [Goes et al., 2009]) is an important species. Groundwater samples however proved the bicarbonate concentration to be equal or higher than the chloride concentration for shallow depth, but an order of magnitude lower for deeper groundwater. The other reason for choosing chloride as the element is the model is due to the fact that chloride is a conservative element: it is non-adsorbent, non-absorbent, non-reactive and decay is very slow. The only factors which are changing the chloride concentration are precipitation and evaporation (which only occurs in the top cells) and advection, diffusion and mechanical dispersion.

7.3 Initial conditions

In order to determine the current day situation of the freshwater lens in the creek ridge, the model was initially made completely saline ([Cl] = 18630 mg/L) and fresh groundwater recharge was simulated using well cells. The chloride concentration on the boundaries was kept constant at 18630 mg/L. The model calculated with transient flow and run for 150 years using stress periods of length 0.5 year until the freshwater lens reached equilibrium. Stress periods alternated between winter stress periods where the net recharge was positive (1.4 mm/day) and summer stress periods where the net recharge was negative (-0.2 mm/day). The chloride concentration of the recharge water was 20 mg/L. The calibrated initial heads were obtained from the Zeeland model [van Baaren et al., 2012]. These heads were initially freshwater heads and had to be converted into saltwater heads for usage in SEAWAT.

Ditches were simulated as river cells and were kept the same as in the model of Visser. They were drawn in ArgGIS and inserted in the model. River conductances were calculated by the model based on the surface area of the ditch and the head in the river [Guo and Langevin, 2002]. Heads in the ditches differ 30 cm between winter and summer stress periods, with higher stages in winter. This results in different river input per stress period. The level controlled infiltration which was used in the infiltration scenario runs was modelled as additional infiltration. The approach is decribed in detail in section 8.3.1.

7.4 Model calibration

7.4.1 Calibration approach

In model was initially completely saline and the desired result was to come up with the current day situation (as of 3rd of July 2013). To come up with the current day situation

a stepwise approach was taken:

1. *Model the equilibrium situation*: In this way, the natural growth of the freshwater lens was simulated until equilibrium was reached. The results (thickness of freshwater lens, heads) were compared to the measurements and if parameter values were adjusted if needed.

2. *Model on small timescales to reach the current day situation*: From the equilibrium situation onward several years (2010, 2011,2012 and 2013) were modelled with actual daily recharge and evaporation data to come up with the exact current day situation as of the 1st of July 2013. The most important results in these runs were the hydraulic heads which were compared and calibrated to the diver data. If needed, parameter values were adjusted again. The model results of the year 2013 run could then be used as a reference simulation to the infiltration run which would be done over the same time period.

7.4.2 Equilibrium situation

The equilibrium situation in the creek ridge has been modelled from initial saline conditions, with freshwater being added by recharge. The model was run until the freshwater lens reached an equilibrium state. This means that the thickness of the freshwater lens in the creek ridge did not change anymore with time. For calibration several model parameters were adjusted for the model to run properly and to get a calibrated equilibrium situation.

Convergence criteria
The head change criterion (HCLOSE) is a convergence parameter which was set to $10^{-6}m$ in the MOCDENS3D model by Visser. The SEAWAT model did not converge with this small value, therefore it was set to a higher value until the model converged. HCLOSE was set to a value of $10^{-5}m$ for the SEAWAT model. The residual convergence criterion (RCLOSE) has units of cubic length per time in MOCDENS3D, but in SEAWAT it has units of mass flux per time. For usage in SEAWAT it had to be increased by a factor equal to the fluid density. Therefore RCLOSE was set to 1.

Solver method
Initial runs were done with a finite difference solver, since this would same time and it is not as memory consuming as other solver methods. However, numerical dispersion is also much larger than by other solver methods. For the final runs, it was needed to find the solver method which would give satisfactory results, but was not too time consuming in run time.

7.4.3 Current day situation

The most important measurements which the model had to be calibrated to were the diver data. Diver data consists of hourly measurements of the groundwater level. Two major adjustments had to be made for the model to run on small timescales, namely the

stress period length and the crop factor.

Crop factor

Groundwater heads were compared to on continuous (hourly) measurements of divers over longer periods. Precipitation , P and evaporation E data were obtained from the nearest Royal Dutch Weather Institute (KNMI) in Vlissingen, about 15 km from the field test. Daily data on recharge, temperature and evaporation (in mm/day) was available, but for simplification the net recharge N was calculated form the difference between P and E (P and E are both positive). Evaporation was dependant on a crop factor C.

$$N = P - C \cdot E \tag{7.4.1}$$

In case N would be a negative, it was set to zero. This calibration step was needed, since largely negative stress periods in the summer would result in a unrealistically deep groundwater level in the creek ridge. The assumption is valid since the groundwater level is already quite deep in summer and the evaporated water would not reach the atmosphere within the stress period length of one day. Water would then effectively not evaporate from the soil within the stress period.

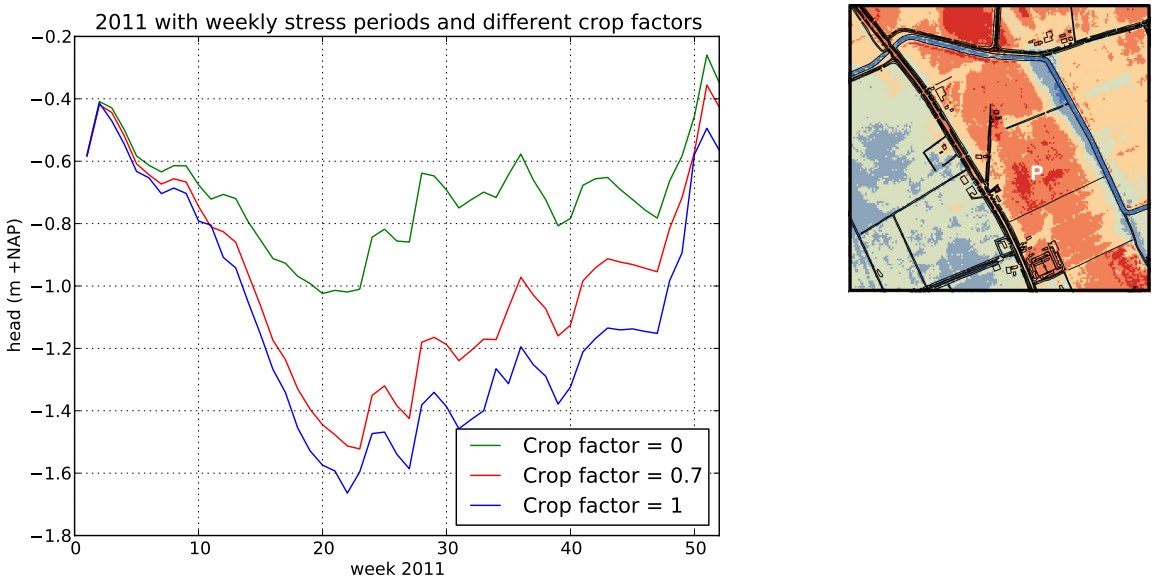

Figure 7.4.1: Modelled hydraulic heads at the Pump through the year 2011 with weekly stress periods and different crop factors

Stress period length

For modelling on finer timescales, the model was checked to have run for one years (2011) with varying stress period lengths: half year, monthly, weekly and daily stress periods. The crop factor was set to zero. The initial head distribution and chloride concentration was obtained from the last output time from the equilibrium situation. For one further adaption step, the year 2010 was used as a adaptation year for the model to adjust to the more accurate hydraulic head distribution. The year was run with weekly stress periods and accurate recharge. The modelled heads and concentration values as of

31st of December 2010 were used as the input for the 2011, 2012 and 2013 runs. From the daily recharge data provided by the KNMI, recharge input files were made with averaged recharge per half year, month and week. The heads calculated by the model in the first cell where the hydraulic head is located within the vicinity of the cell. In the top cells of a row/column the heads are often located beneath the bottom of the cells. The obtained heads as well as the diver data collected in 2011 and 2012 are plotted in figures 7.4.2 and 7.4.3.

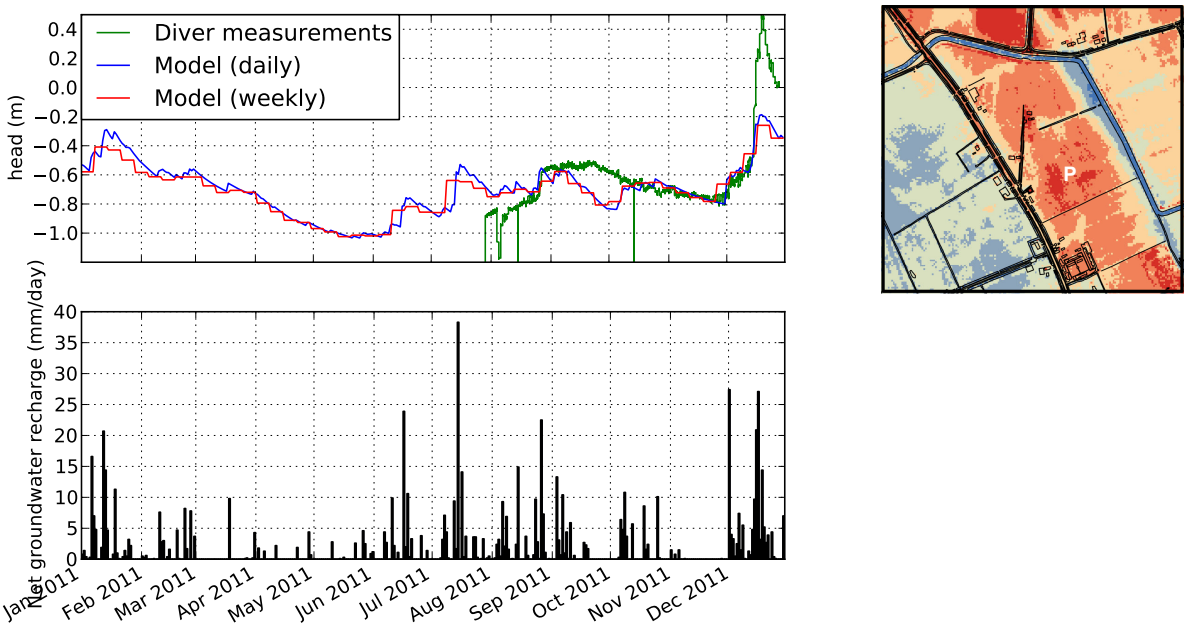

Figure 7.4.2: Hydraulic heads in the cell where the groundwater level is located at the location of the Pump in the year 2011. The year is modelled with different stress period lengths. The red graph gives the hydraulic head with weekly stress periods, the blue graph gives the hydraulic head with daily stress periods and the green graph is the measured diver data. The lower graph gives the daily groundwater recharge using a crop factor of 0.

It is obvious that daily stress periods give the most accurate approximation to the diver data, although there is still an difference with the calculated model heads, especially in the times of high recharges (December 2011). In order the obtain the exact current situation (as of the 3rd of July 2013), the model was run with daily stress periods for the years 2011, 2012 and 2013 (until 3th of July). Since infiltration started as of 21st of May 2013, the model is run twice for the period of 1st of April until 3th of July 2013 , one run including infiltration and one run excluding infiltration.

7.5 Sensitivity analysis

In order to determine the sensitivity of the model to changes in input parameters, several calibration runs have been performed. The input for the model was exactly the same as for the equilibrium situation run, but each time one parameter was changed. To compare the results to the equilibrium model run, the chloride concentration is plotted for the location

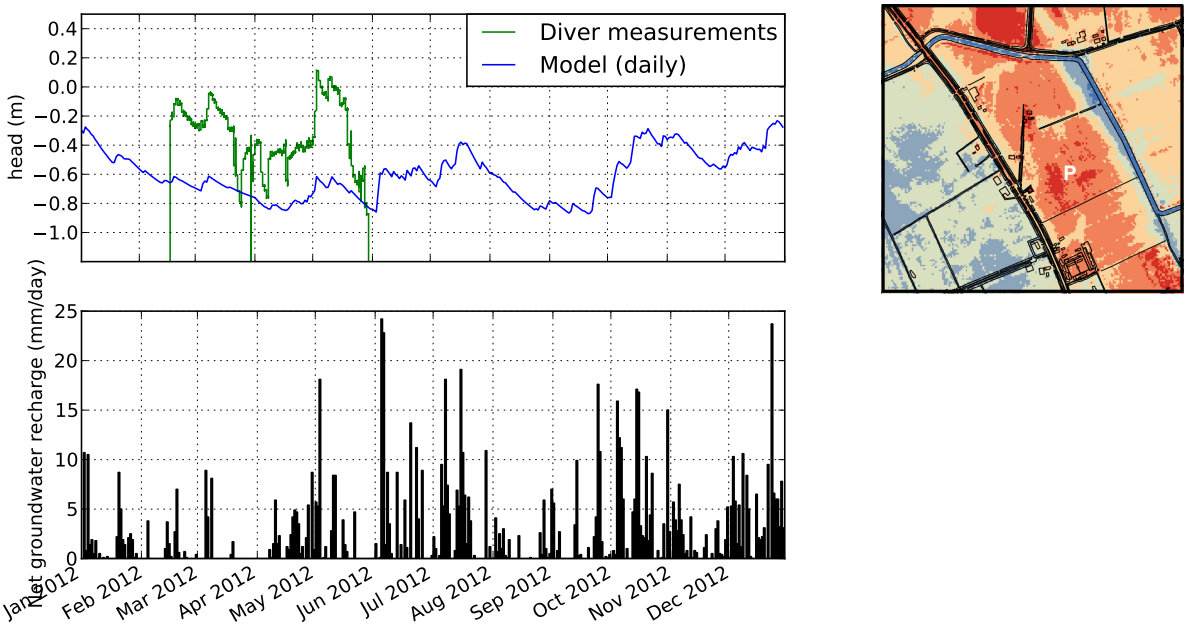

Figure 7.4.3: Hydraulic heads in the cell where the groundwater level is located at the location of the Pump in the year 2012. The blue graph gives the hydraulic head with daily stress periods and the green graph is the measured diver data. The lower graph gives the daily groundwater recharge using a crop factor of 0.

of the pumping well since this is closed to the maximum thickness of the freshwater lens. Both sensitivity on dispersion parameters (dispersivity and diffusion coefficient) as well as convergence and numerical parameters (Courant number, head conversion criteria and different solver methods) were investigated.

The sensitivity was compared at the locations where most measurements were available. These locations are Minifilters I and Minifilters II on the property of Sanderse and Pumping well on the location of Louwerse. The concentrations have been plotted in depth profiles. In each plot the blue line is the standard, calibrated concentration, the red iness are the concentrations calculated with the changed parameter value given above the graph. The red dots are the chloride concentration values measured in the lab by ICP-OES and the green dots are the chloride concentrations calculated out of the in situ measured EC values by the EC-concentration given by Goes [Goes et al., 2009].

In most of the plots red and blue lines look very similar and are on top of each other. This means that a coarser number of the given parameter is justified in this case. This is the case for the higher Courant numbers and the higher head closure criterium hclose. This not the case for the dispersivity parameters. Increasing α_l to 1 m drastically increases dispersion. A smaller α_l (0.01 m) on the other hand increases the accuracy of the calculated concentrations to the measured choride values. The same holds for setting the diffusion coefficient to zero, effectively neglecting diffusion. The thickness of the mixing zone is slightly reduced in both plots as well.

Finally, when looking at the solver methods it can be seen that there are no significant differences between using the MOC method or the HMOC method. The TVD graph on the other hand is significantly different from the HMOC graph. The TVD calculates

a thicker freshwater lens up to 12.5 m depth at all locations. The mixing zone is also thinner. However, this does not match with the measurements and therefore the HMOC method is better in this way.

Table 7.5.1: Sensitivity analysis

Parameter	Unit	Default value	Changed values		
Longitudinal dispersitivy	m	0.1	-	0.01	1
Molecular diffusion coefficient	mol^{-1}	$8.64 \cdot 10^{-5}$	-	-	0
Courant number	[-]	1	0.75	2	4
Head conversion criterium	mm	0.1	-	0.01	1
Solver methods	-	HMOC	-	MOC	TVD

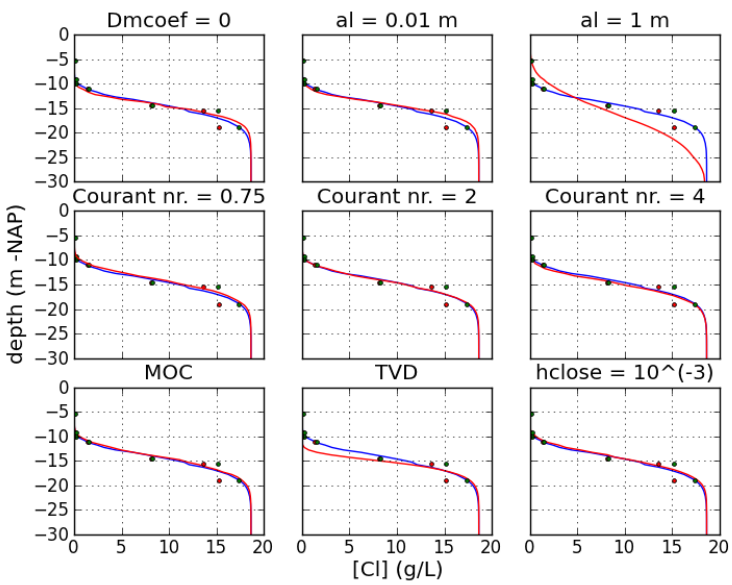

Figure 7.5.1: Depth profiles of the chloride concentration (g/L) in Minifilters I. The blue graphs represent the calibrated 'normal' concentrations, the red lines represent the concentrations calculated with the different parameter value. The red and green dots are the chloride concentrations of the ICP-OES analysis and chloride concentrations calculated from EC values respectively. Default values for Dmcoef, α_l, Courant number, HCLOSE and the solver method are found in table 7.5.1

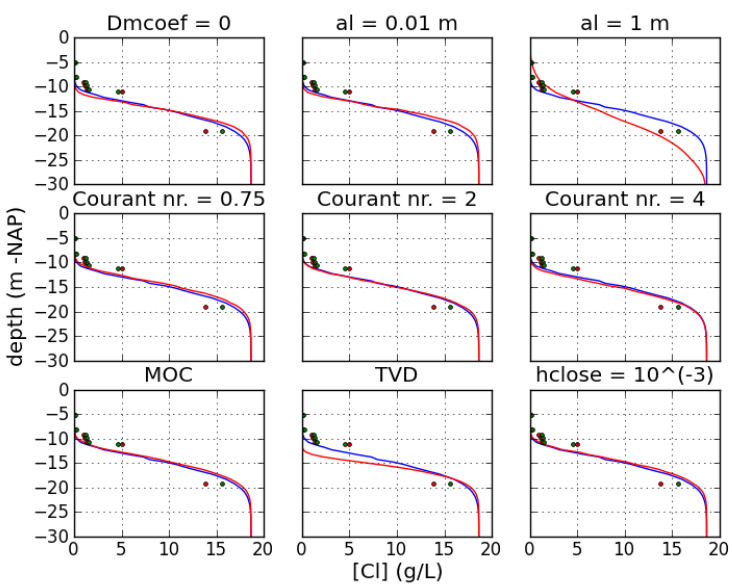

Figure 7.5.2: Depth profiles of the chloride concentration (g/L) in Minifilters II. The blue graphs represent the calibrated 'normal' concentrations, the red lines represent the concentrations calculated with the different parameter value. The red and green dots are the chloride concentrations of the ICP-OES analysis and chloride concentrations calculated from EC values respectively. Default values for Dmcoef, α_l, Courant number, HCLOSE and the solver method are found in table 7.5.1

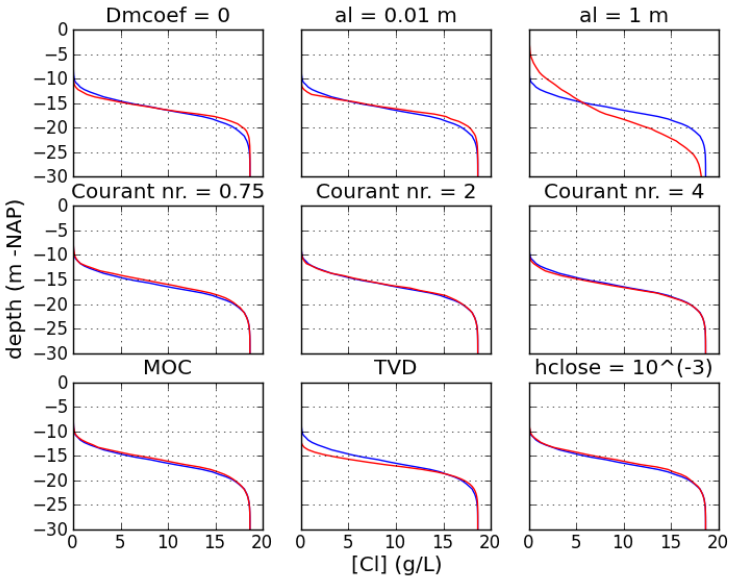

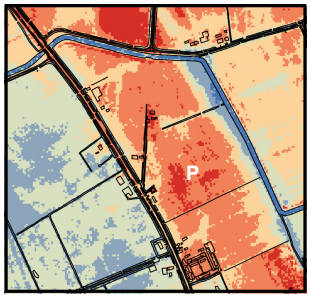

Figure 7.5.3: Depth profiles of the chloride concentration (g/L) in Pumping Well. The blue graphs represent the calibrated 'normal' concentrations, the red lines represent the concentrations calculated with the different parameter value. The red and green dots are the chloride concentrations of the ICP-OES analysis and chloride concentrations calculated from EC values respectively. Default values for Dmcoef, α_l, Courant number, HCLOSE and the solver method are found in table 7.5.1

8. Model Results

8.1 Equilibrium situation

Since freshening of the aquifer means the total mass of saline waters M will decrease with time, the ratio $\frac{M}{M_0}$ (where M is the total mass of water in the model domain at any time t and M_0 is the initial mass in the domain at $t = 0$) will decrease as well and with be at a constant level when equilibrium has been reached. Perfect equilibrium is not reached, since M is the total mass in the model domain which also includes other areas than the creek ridge. Infiltration may still occur there, but since this is not within the area of interest, the system is assumed to be at equilibrium.

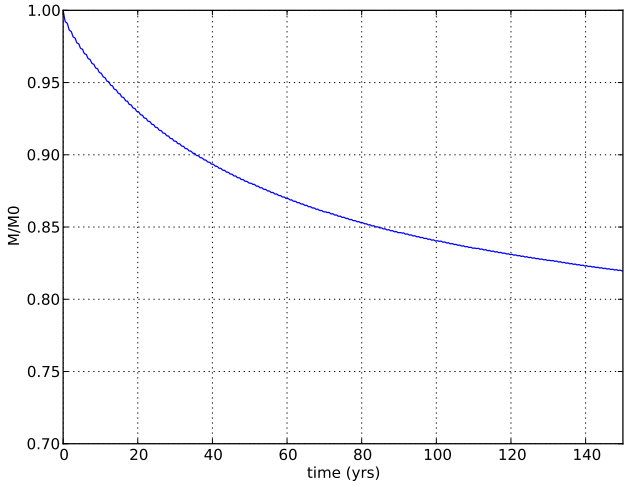

Figure 8.1.1: Total mass M in the domain normalized to the initial total mass M_0 during the time to equilibrium. Equilibrium of total mass is not reached within 150 years, however this is due continuous infiltration in areas of the domain apart from the creek ridge. Equilibrium in the creek ridge is reached at roughly $t = 150$ yrs

The next figures show the equilibrium situation in three different ways: (1) 2D contour plots, (2) time series at measurement locations and (3) cross sections.

2D contour plot
Figure 8.1.2 shows the 2D contour plots of two levels of chloride concentration (150 mg/L and 1000 mg/L). These levels were chosen, because they represent the maximum values for fresh and brackish water (table 5.3.1). On the property of Sanderse, the maximum depth to the fresh-brackish interface was found to be at elevations of 10 - 11 m -NAP according to the EC-measurements, Slimflex, sample analysis and SMD (figure 6.2.1, figure 6.3.1, table 6.4.1 and figures 6.5.1/6.5.2). The red areas are either ditches which are brackish or areas with lower surface level elevation. The brackish water ditch to the north of the property of Sanderse causes the lens on the property of Sanderse to be smaller since upconing of saline groundwater seems to occur under the ditch.

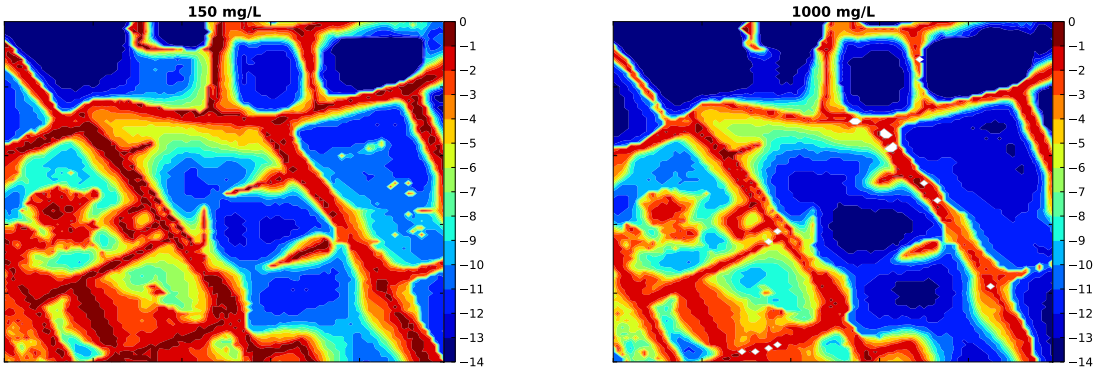

Figure 8.1.2: Elevation (m) of the 150 mg/L chloride concentration contour (left) and the 1000 mg/L chloride concentration contour (right). Given elevations are relative to NAP.

Time series at measurement locations

The depth of the freshwater lens at the various locations of the monitoring were calculated and plotted as a function of time. The system was assumed to be at equilibrium after 150 years. The depth to the fresh-salt interface on locations Minifilters I and Minifilters II is calculated to be 10 m - NAP, which is equal to the depths observed by the groundwater sample analysis, the EC measurements of pumped up groundwater and the EC measurements by the SMD. CVES transect C, which runs close to Minifilters I, shows a thickness of the freshwater lens of 10 m as well. CVES transect A-B runs through Minifilters III, Minifilters II and Minifilters I respectively. In Minifilters III the model shows that at that location no freshwater is present. The is confirmed by both CVES transect A-B and the EC measurements done in Minifilters III. Only high EC values were measured there.

The timeserie at Slimflex D shows a large mixing zone between the 150 mg/L contour and the 1000 mg/L contour.

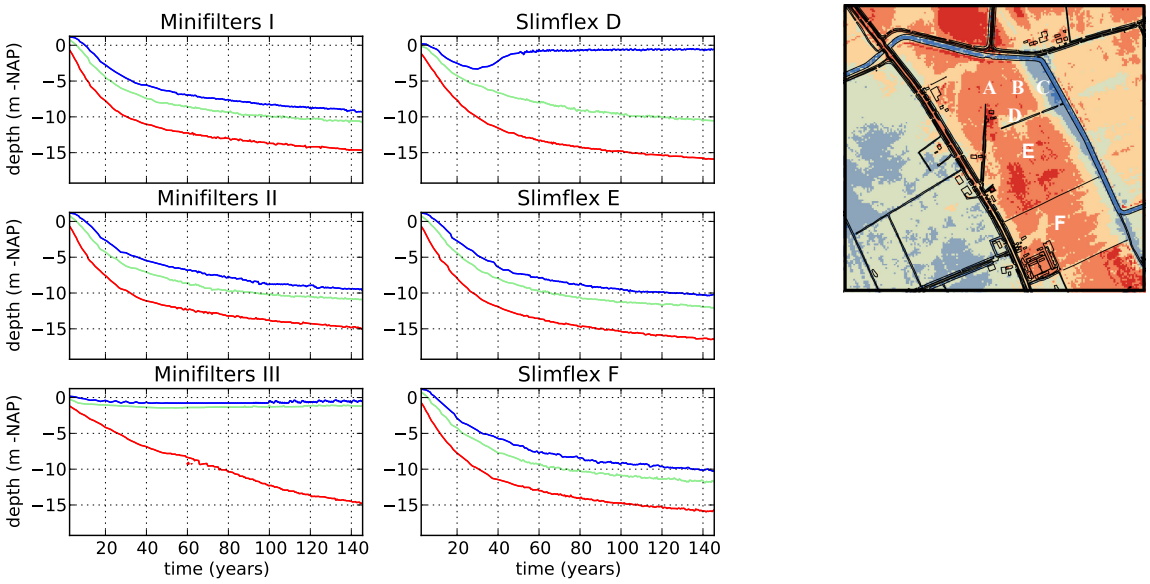

Figure 8.1.3: Depth of the freshwater lens as a function of time at locations I, II, II, D, E and F. The lines represent points of equal chloride concentration: Blue: [Cl] = 150 mg/L, Green: [Cl] = 1000 mg/L and Red: [Cl] = 10000 mg/L. All the water above the blue line can be considered as completely fresh, while the water in between the red and green line is considered brackish.

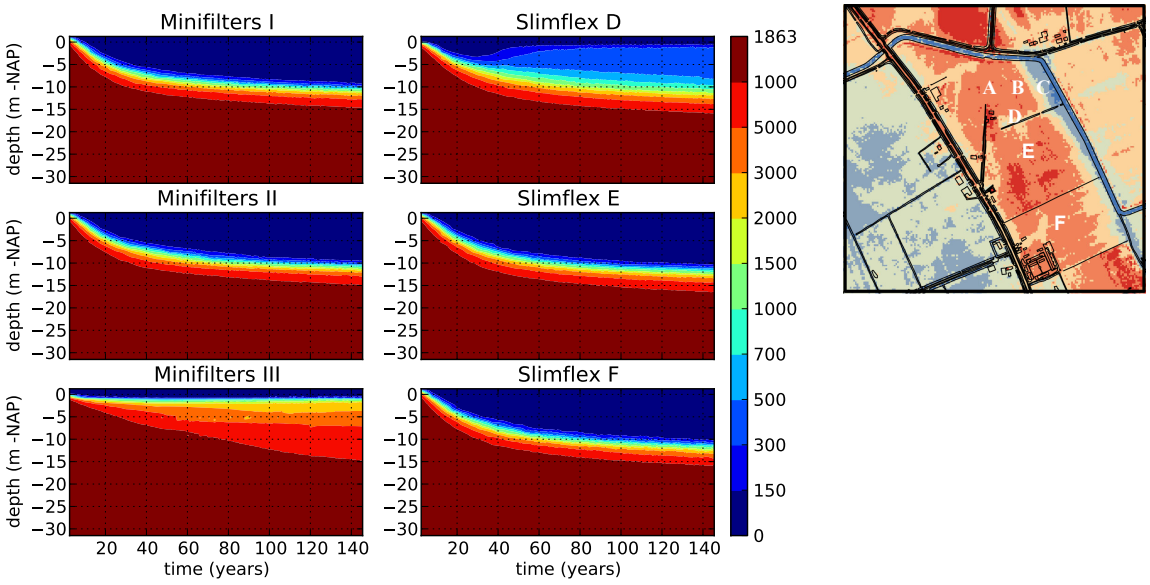

Figure 8.1.4: Chloride concentration (in mg/L) as a function of time contour plot of the thickness of the freshwater lens at locations I, II, II, D, E and F

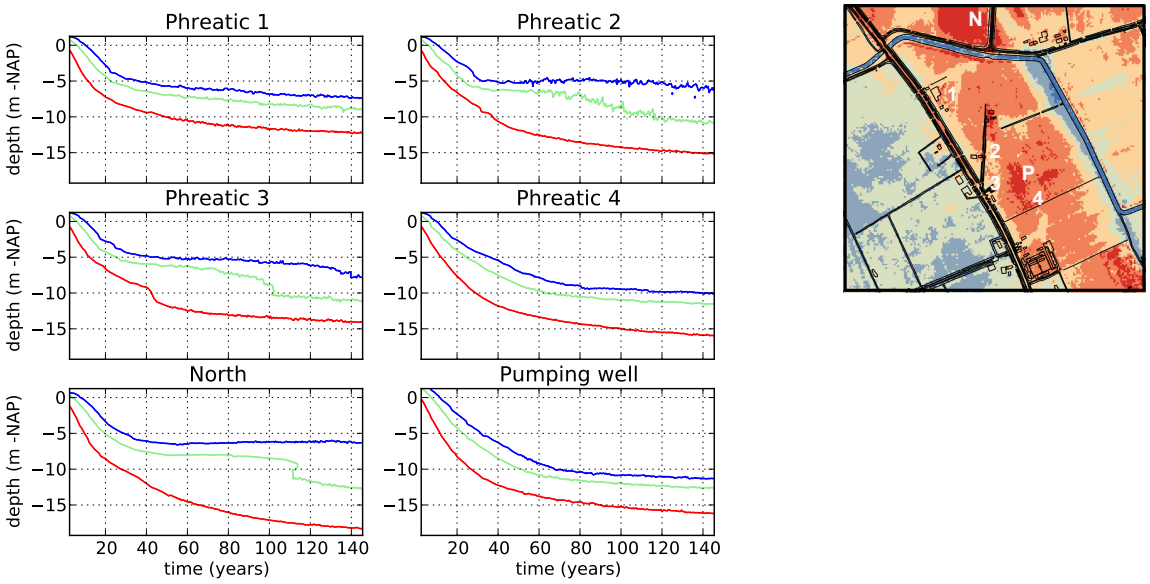

Figure 8.1.5: Depth of the freshwater lens as a function of time at locations 1, 2, 3, 4, N and P. The lines represent points of equal chloride concentration: Blue: [Cl] = 150 mg/L, Green: [Cl] = 1000 mg/L and Red: [Cl] = 10000 mg/L. All the water above the blue line can be considered as completely fresh, while the water in between the red and green line is considered brackish.

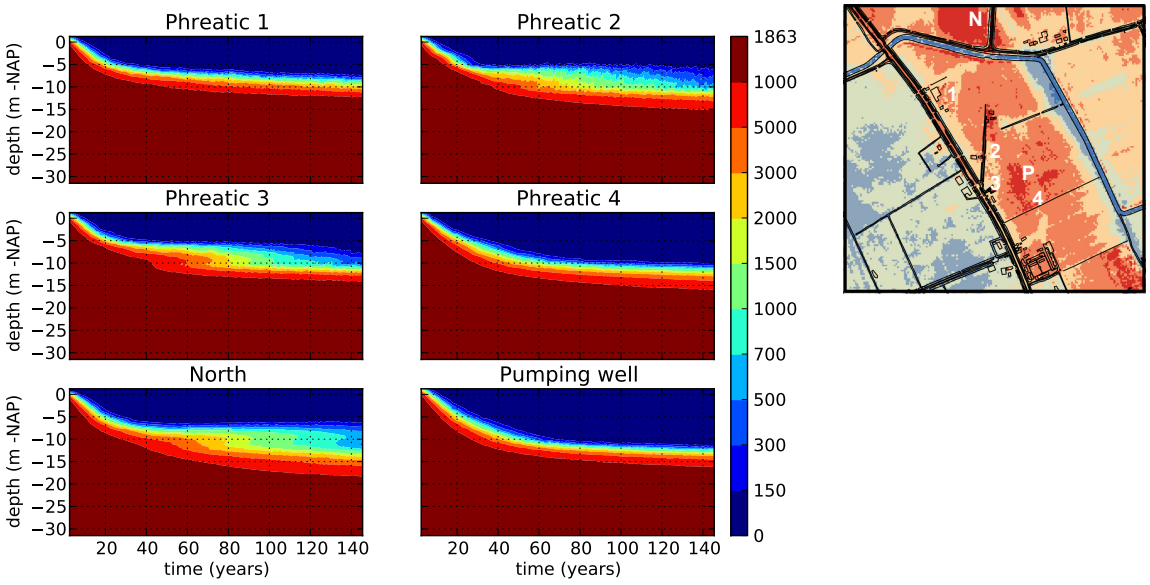

Figure 8.1.6: Chloride concentration (in mg/L) as a function of time contour plot of the thickness of the freshwater lens at locations 1, 2, 3, 4, N and P

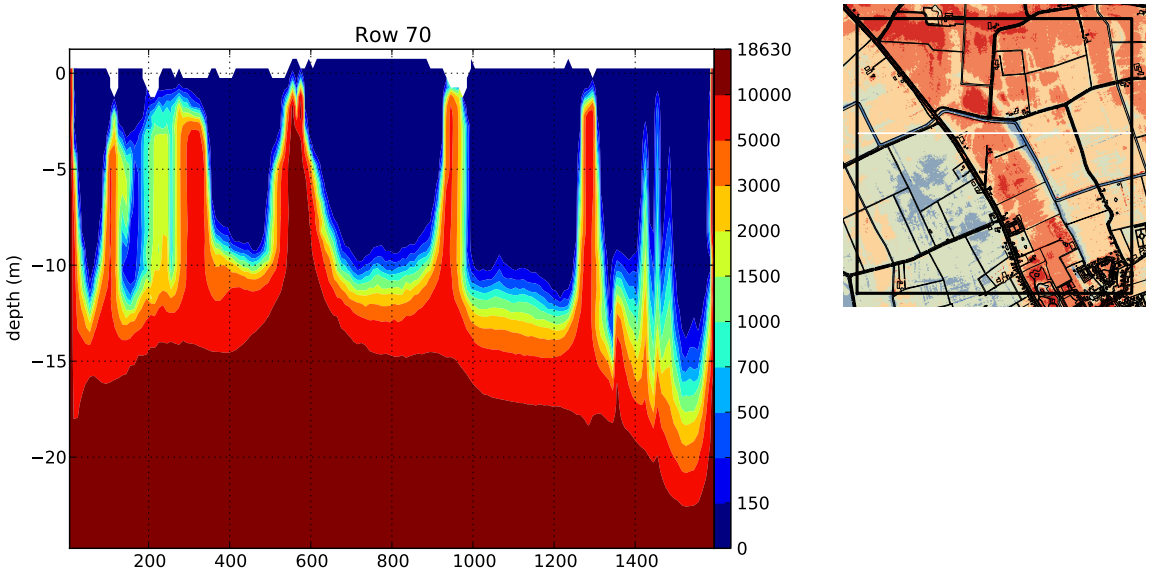

Figure 8.1.7: Chloride concentration (in mg/L) contour plot of the equilibrium situation in row 70 of the model.

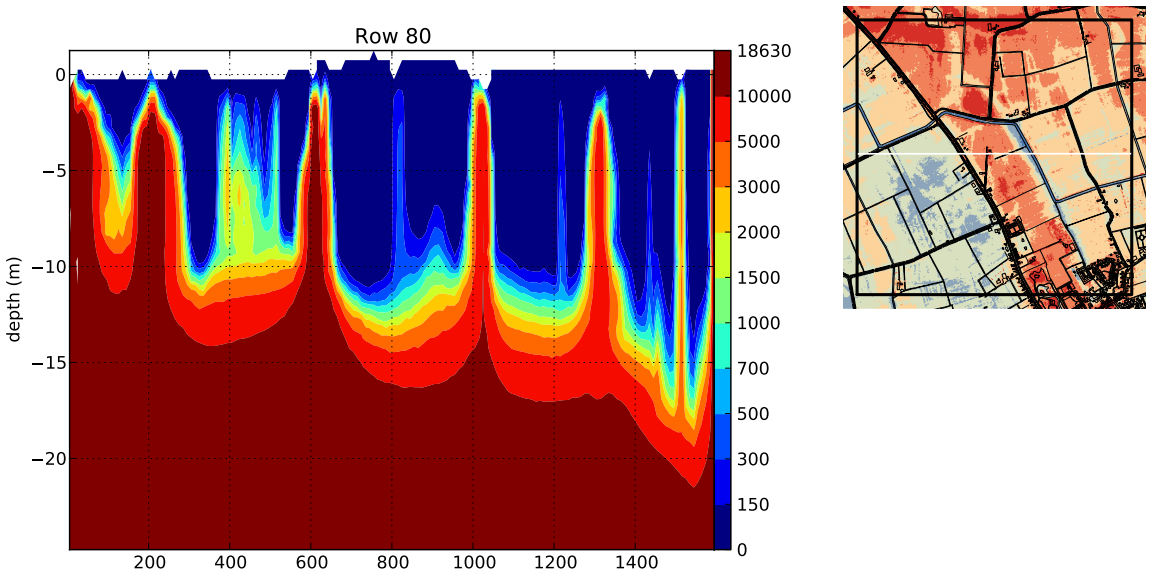

Figure 8.1.8: Chloride concentration (in mg/L) contour plot of the equilibrium situation in row 80 of the model.

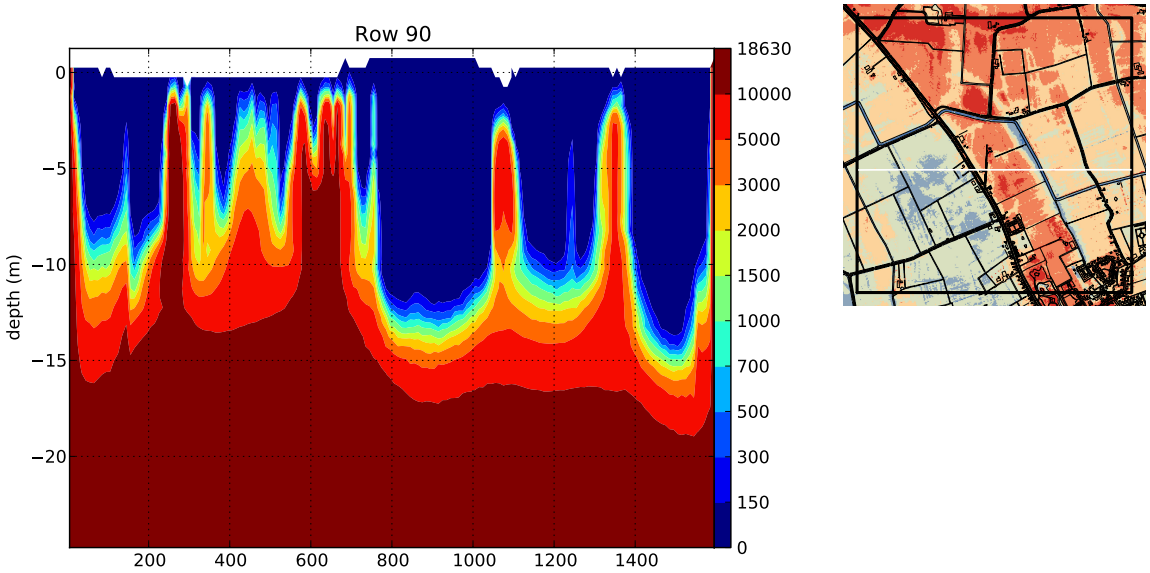

Figure 8.1.9: Chloride concentration (in mg/L) contour plot of the equilibrium situation in row 90 of the model.

Cross sections

Three plots have been made of transects along the creek ridge. These are row 70 (figure (7.4.7)), row 80 (figure (7.4.8)) and row 90 (figure (7.4.9)) of the model. The creek ridge is located between the points $x = 600$ and$x = 1000$ in all three plots. For figure 7.4.7, the transect runs along the creek ridge along the line of Minifilters I, II an III. Minifilters I is located at $x = 800$, Minifilters II is located at $x = 850$ and Minifilters III is located at $x = 950$. The freshwater lens reaches to around 10 meters depth. The thickness of the mixing zone is several meters. The model also calculates freshwater lens left and right of the creek ridge. This is not verified in the fiels, but since they are not particularly in the fiels of interest, it is not investigated further. Upconing seams to be compared to surface level elevation and the presence of ditches. At $x = 200$, the land surface level is 1 m lower than the surrounding area, and this has a siginificant effect.

The second transect is of row 80 of the model (figure (7.4.8)). This transect runs across the creek ridge and crosses the ditch that seperates the properties of Louwerse and Sanderse as well. The upconing at $x = 825$ is caused by the ditch, which is also visible by the lower surface elevation there. If we look at the area west of the creek ridge, it can be seen again that just like in the plot of row 70, the surface elevation is an important factor for the thickness of a freshwater lens. The surface elevation is only slightly higher at $x = 300$ compared to the point $x = 500$, but apparently this is enough to form a freshwater lens of several meters. Again, this has not been verified with field measurements.

The third transect runs across the middel of the property of Sanderse and here the deepest point of the freshwater lens would be located here. That is the point $x = 900$ which indeed shows a depth of the freshwater lens of around 13 m, which is slightly shallower than measured in CVES transect B (6.1.3).

8.2 Climate scenario's

To model the effects of climate change as proposed by the Royal Dutch Meteorological Instute (KNMI) several scenarios are most likely to happen in the near future in the Netherlands. These ideas were proposed in 2006 [Voortman, 2010]. The 4 different scenarios are given in table 8.1.1.

Table 8.2.1: Names and causes climate scenarios proposed by the Royal Dutch Weather Institute [Voortman, 2010]

Climatescenarios accoring to the KNMI (2006)

Scenario code	Effects
G	No change in air currents and temperature increase of 1 degree C
G+	Changes in air currents and temperature increase of 1 degree C
W	No change in air currents and temperature increase of 2 degree C
W+	Changes in air currents and temperature increase of 2 degree C

Changes in precipitation and evaporation for the 4 different climate scenarios according to the KNMI were obtained for the year 2050 (KNMI website). From these recharge rates new recharges rates were calculated based on the base recharge rates of 1.4 mm/day in winter and -0.2 mm/day in summer. New recharge rates are given in table (8.1.2).

Table 8.2.2: Recharge rates in climate scenario run

Scenario	Recharge rate Winter	Recharge rate (Summer)
Control	1.4	-0.2
G	1.453	-0.208
G+	1.525	-0.562
W	1.517	-0.216
W+	1.661	-0.924

These recharge rates represent the net recharge in the year 2050. Equilibrium was assumed to be around the year 2000, so the model had to be run for 50 years. The change in net recharge to the net recharge in 2050 was assumed to be linear and the recharge input was calculated to be as such. The model was then run once for G, G+, W and W+ and output was made for the middle of the creek ridge on the property of Louwerse, since it was expected that the maximum change would be observed there. To compare the effect of climate change, the model was also run another 50 years with the normal recharge rates of 1.4 mm/day in winter and -0.2 mm/day in summer. This was done to prevent a possible effect of the model to not be at equilibrium yet. The change in depth to the fresh-brackish-saline water interface could then be compared to the normal trend. In order to quantify the impacts on freshwater availability, the initial volume of freshwater was calculated. All the cells with a concentration lower than 1500 mg/L were counted, the volume of the cell was calculated and corrected for porosity. The reason for

choosing 1500 mg/L was decided, because that is according the farmers the maximum allowed workable concentration of chloride for irrigation.

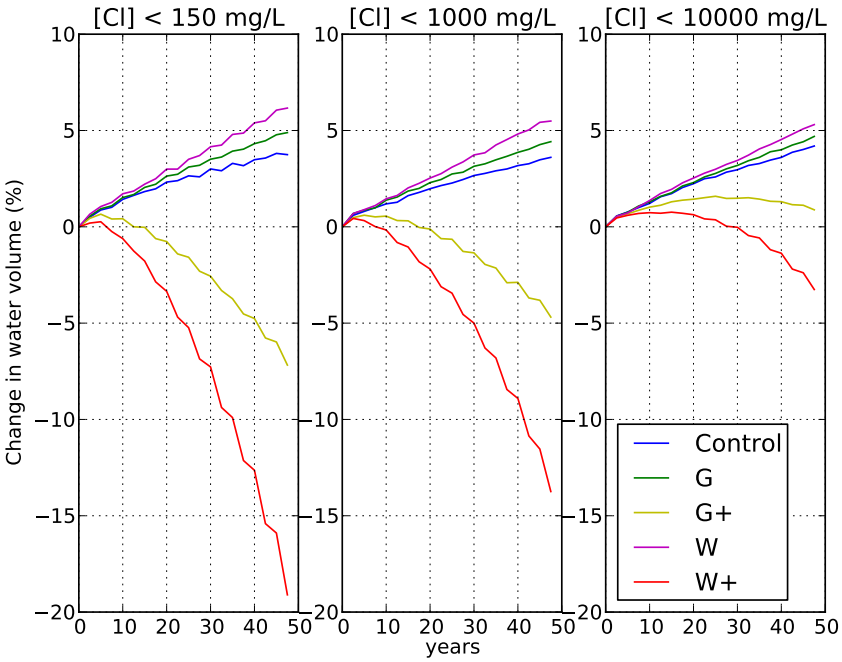

Figure 8.2.1: Percentual change in freshwater availability according to climate scenarios G, G+, W and W+. A Control run was also done to check the state of equilibrium in the creek ridge. Since the total mass in the creek ridge is still increasing, the system was not entirely in equilibrium yet.

According to the Control run, the total freshwater mass in the creek ridge is still increasing if the model is runned longer. This would mean that this influences the magnitude of change on the scenarios. The effect of the climate scenarios is thus partly influenced by the system not being entirely at equilibrium. If the system would have been at equilibrium, the Control graph would approximately have been at horizontal line at $y = 0$. Percentual changes for all climate scenarios would have been lower (more negative), and so the effect of climate would have been larger. However, even with this limiting effect, the percentual changes according to scenarios G+ and W+ are quite large, with W+ have to most extreme effect of a lowering of the total freshwater volume by 13 percent. Correcting for the system not being at equilibrium would result in a effect of -17 percent in 50 years. The G+ scenario shows a decrease of total fresh water volume by 4 percent, or 8 percent if corrected. Both scenarios G and W show actually as small increase in total freshwater volume.

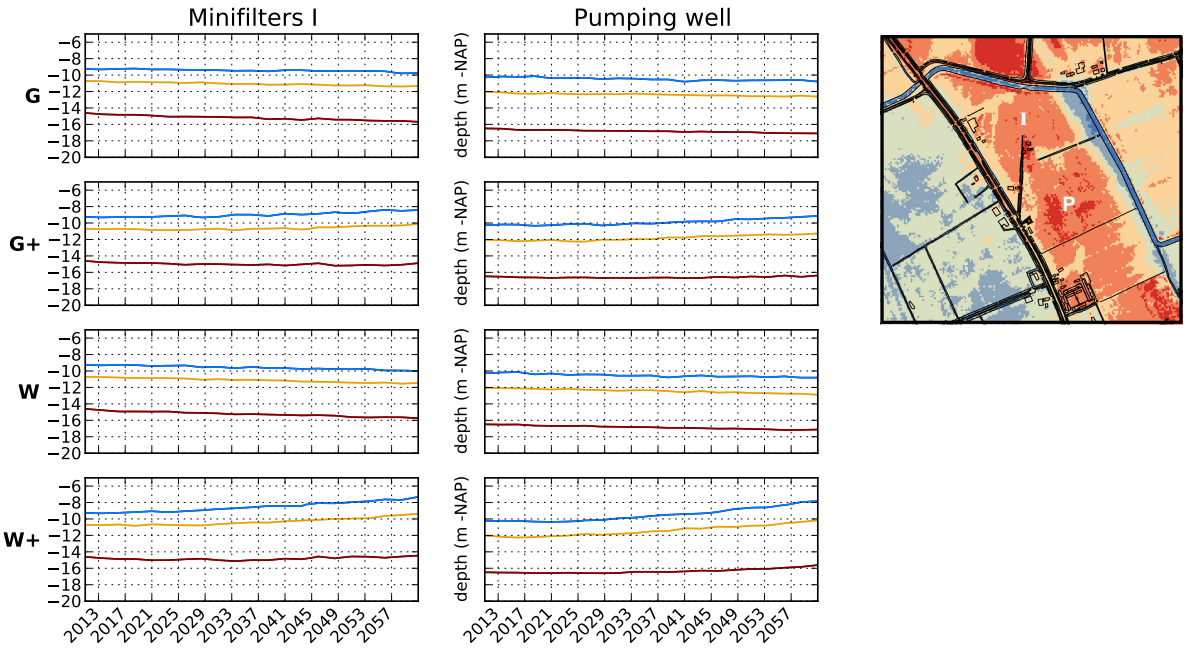

Figure 8.2.2: Time series of the depth of certain chloride concentration contours as a result of the corresponding climate scenario. The row determines the climate scenario, while the column shows in at which location the results are modelled. The blue contour equals 150 mg/L, the yellow contour equals 1000 mg/L and the red contour equals 10000 mg/L

The 2D contour plots in figure 8.2.3 show the effect on the freshwater lens in 2050. Only the scenarios G+ and W+ are given since it is apparent from figure 8.2.1 that there will be no negative effects for climate scenarios. By comparing the elevations of the 150 mg/L contour of the equilibrium situation to the situation in 2050, we observe that the 150 mg/L contour is located approximately 1 m higher for scenario G+ and 2 m higher for scenario W+. The same holds for the 1000 mg/L contour. This would mean that the freshwater lens becomes 1 or 2 m thinner for scenario G+ or W+. This is can also be concluded from 8.2.2, where it is found that the distance inbetween the 150 mg/L and the 1000 mg/L contour stays the same in time. The distance inbetween the 1000 mg/L contour and the 10000 mg/L contour increases in time however. This can be due to smearing effects, where salt is smeared out if it is transported.

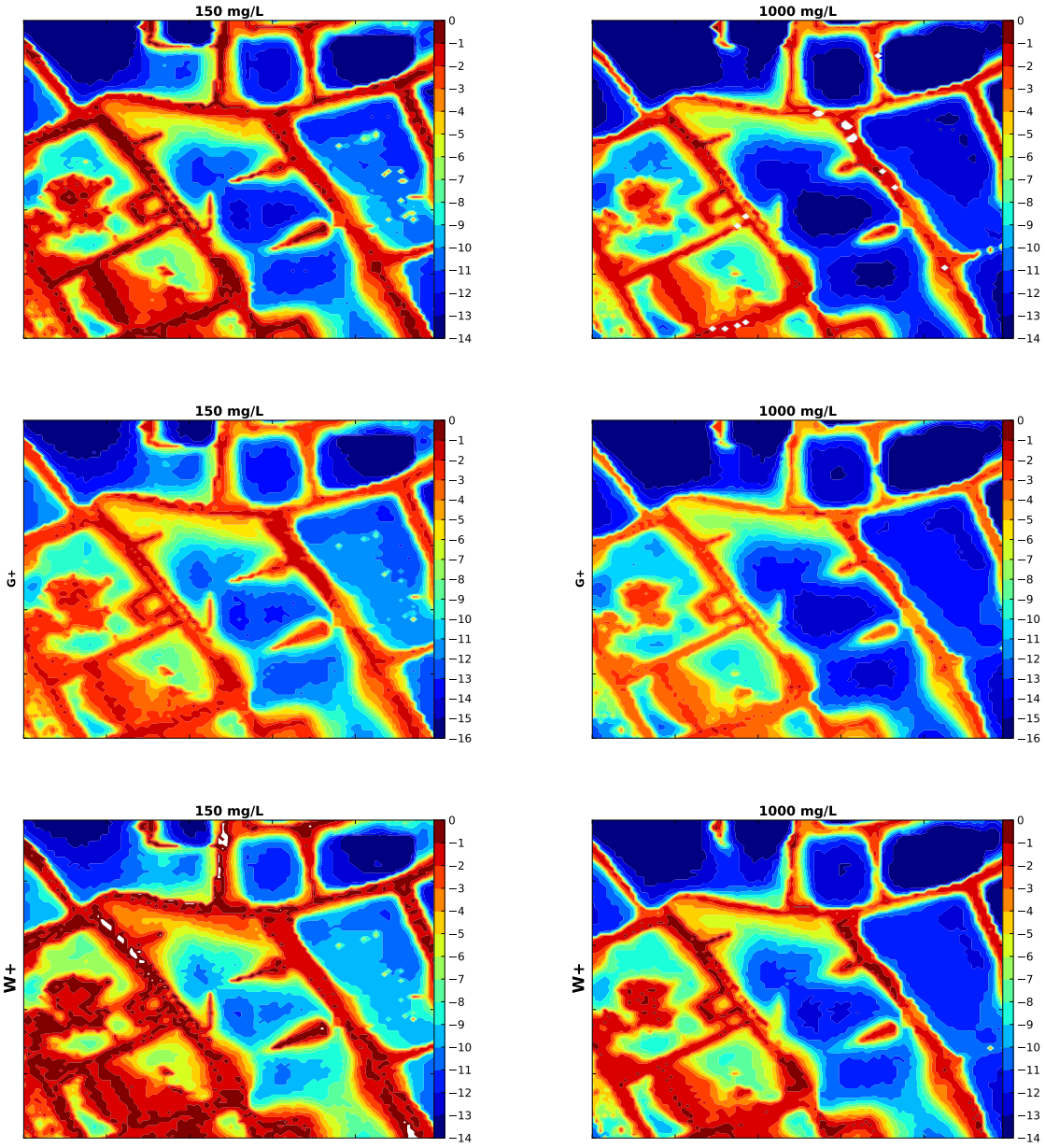

Figure 8.2.3: Elevation (m) of the 150 mg/L chloride concentration contour (left) and the 1000 mg/L chloride concentration contour (right). Given elevations are relative to NAP. The top two plots represent the equilibrium situation, the middle two the situation for climate scenario G+ after 50 years and the bottom two the situation for climate scenario W+ after 50 years.

8.3 Implemented level controlled drainage

8.3.1 Long timescale effect

One of the biggest questions in this paper is to determine the effect of using level controlled infiltration. Because the farmers are most interested in the effects for the near future, it was decided to model the effects for 20 years using stress periods of half year length. The drainage system was drawn in ArcGis. The template from the draineur was used as a reference model. To model the extra infiltration, several options were available. The first option was to introduce an extra constant infiltration flux. This would have been done with adding recharge cells to the drainage system cells. However, since it is not known how large this flux would have to be and it is not possible to quantitively measure this, this is idea was rejected. Therefore the level controlled drainage was modelled as river cells which were given a constant head for the infiltration period. This option is logical since effectively increasing the hydraulic head is what is actually being done in the field test. Moreover, the heads which had to be applied are known from the diver data and the experience of the farmers. Stress periods alternated between 'winter' stress periods including infiltration and 'summer' infiltration where no infiltration is occuring and the river cells which corresponded to level controlled drainage during 'winter' were set to be regular cells. Normal recharge rates were maintained and apart from the addition of the river cells, no adjustments to the base model were made.

According to the farmers the highest manageble controlled level possible on the fields is 50 cm beneath surface level. Setting the controlled level higher would drastically wetten the soil. Because it is highly unlikely for this level be kept constant for longer time periods, it was chosen to model the infiltration period of 20 years for several scenarios: (1) level = 50 cm beneath surface level, (2) level = 75 cm beneath surface level and (3) level = 1 m beneath surface level. Scenario 1 would give the maximum possible effect of the infiltration experiment and would give the 'best case' results, while the 2nd and 3rd scenario give more realistic values for the average controlled level and would therefore give more realistic effects.

Plotting the results was possible in many different ways, but it was chosen to give indication of the thickness of the freshwater lens on both the properties of Sanderse (Minifilters I) and Louwerse (Pumping well). In addition to these locations the results were also plotted for Slimflex F. Because overal groundwater flow is from the dunes in the North-East to the South-East, it is expected that some infiltrated water will flow away from the creek ridge. This portion of the infiltrated water could be considered as 'lost', if it is not pumped up in time.

As can be seen from figure 8.3.1, the biggest changes in the thickness of the freshwater lens are observed in the first years after infiltration started. Fluctuations are visible which are caused by the lack of infiltration in summer. When infiltration stops, the head on the fresh-salt interface is increased compared to the head in the top of the soil. The results for scenarios (1) and (2) look very similar. On the property of Sanderse the system will reach an equilibrium state again where the thickness of the freshwater lens will be around 25 m beneath NAP. The thickness of the lens will have increased by 15 m. On the property of Louwerse, the same thickness of the freshwater lens is observed, however for scenario (1) the thickness of the lens seems to increase again after a state of equilibrium

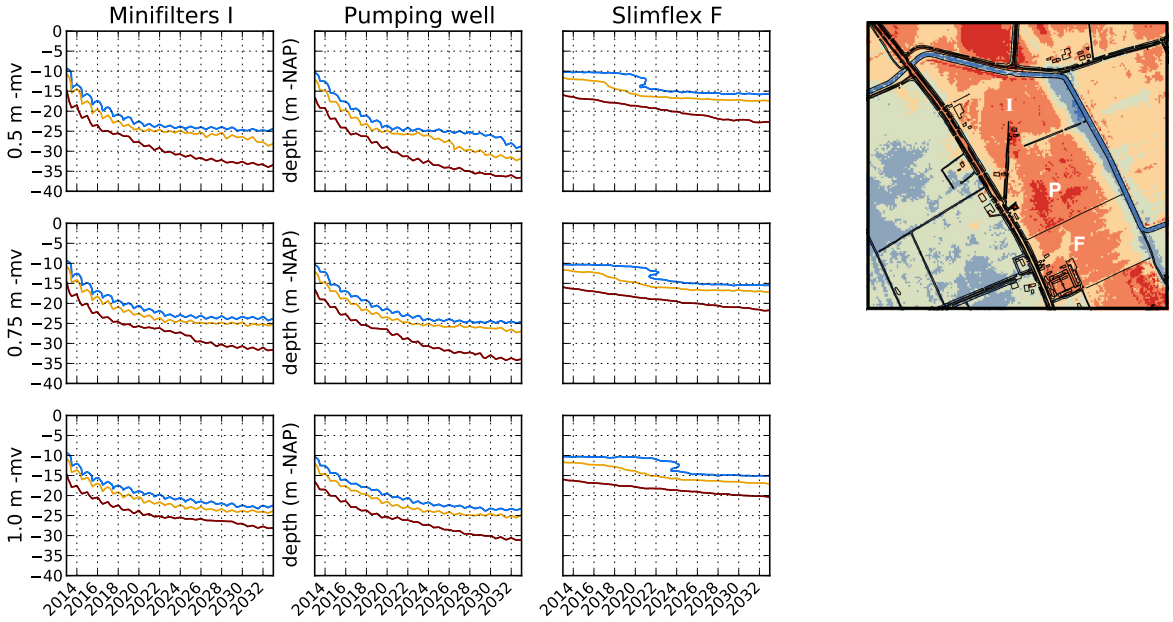

Figure 8.3.1: Depth of the freshwater lens as a function of time during 20 years of infiltration. Results are plotted for 3 locations (Minifilters I, Pumping well and Slimflex F) for the three scenarios. Minifilters I represents effects on the property of Sanderse, Pumping well represents the effects on the properties of Sanderse and Slimflex F would be a reference situation. The blue lines represent the levels with a chloride concentration of 150 mg/L, the yellow lines represent levels with a chloride concentration of 1000 mg/L and the red lines represent the lines with a chloride concentration of 10000 mg/L.

in the 2030. An equilibrium state appears to have been reached as of the year 2020 for scenarios (1) and (2). Scenario (3) shows similar results compared to (1) and (2) with a slightly smaller depth to the fresh-salt interface of 23 m beneath NAP. It also shows lower dispersion effects. If one would define the dispersion as the distance between the concentration lines of 150 mg/L (the blue lines) and 10000 mg/L (the red lines), the smallest distances are observed for scenario (3) and the biggest differences for scenarios (1) and (2).

To look at the effect of groundwater flow, the results for Slimflex F were also plotted. It appears that some freshwater eventually reaches this location after several years. The freshwater lens in thickness by about 5 meters. It also appears that the higher the level of water in the creek ridge, the earlier the water reaches Slimflex F. For scenario (1) the infiltration water front reaches Slimflex F in 2021, for scenario (2) the water front reaches Slimflex F in 2022 and for scenario (3) the water front reaches Slimflex F in 2024. Theoretically this makes sense since the head difference between the head in the creek ridge and the head at the location of Slimflex F is highest in scenario (1), after that scenario (2) is highest and so on. The overall flow velocity towards Slimflex F is than also highest for scenario (1). Therefore, the infiltration front reaches Slimflex F in scenario (1) the earliest.

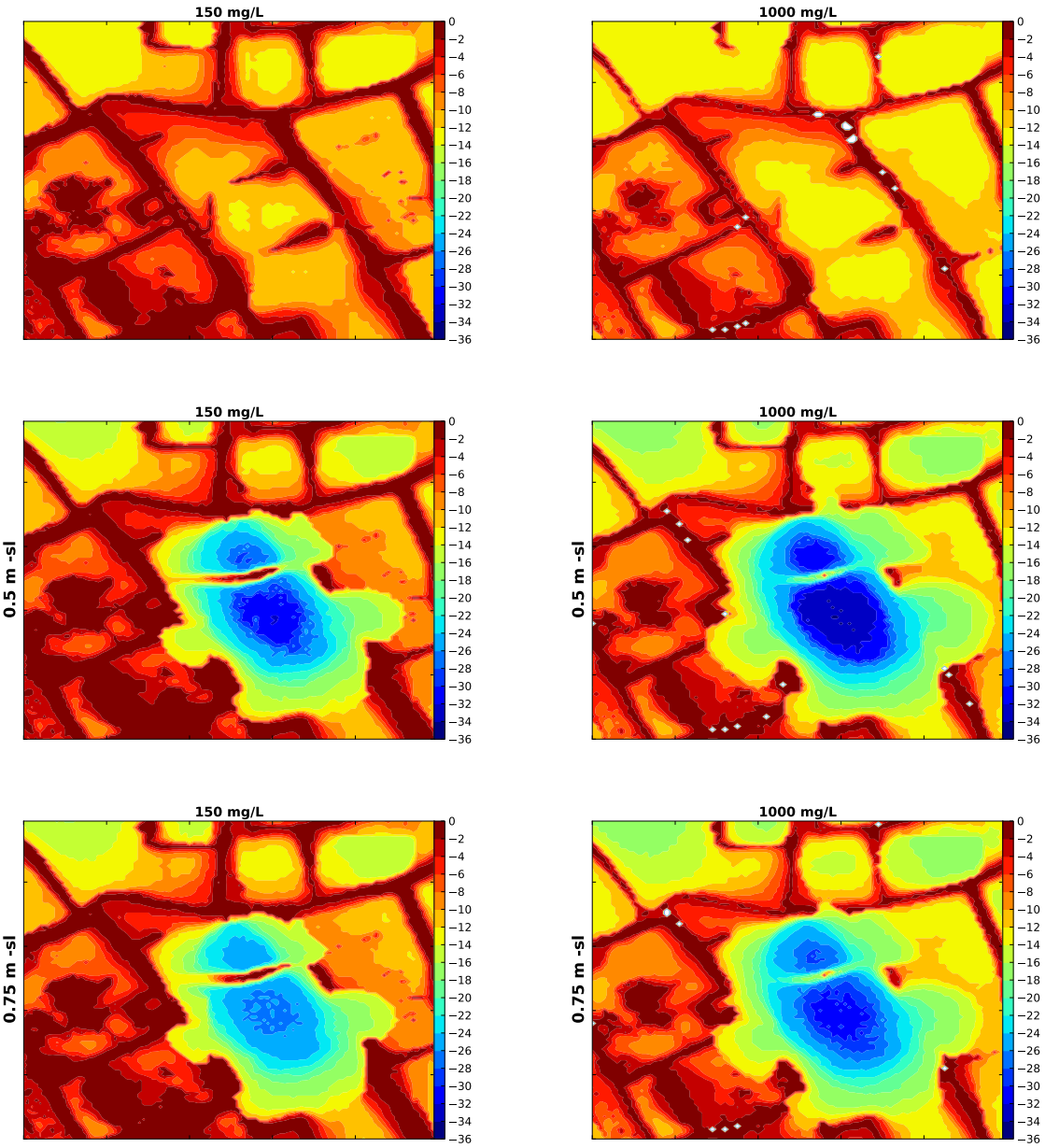
150 mg/L
1000 mg/L
0.5 m -sl
0.75 m -sl
0
−2
−4
−6
−8
−10
−12
−14
−16
−18
−20
−22
−24
−26
−28
−30
−32
−34
−36

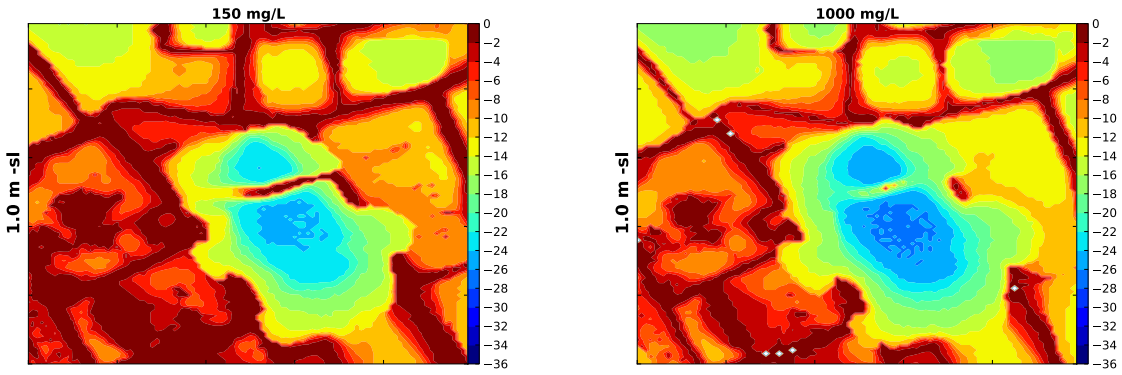

Figure 8.3.2: Elevation (m) of the 150 mg/L chloride concentration contour (left) and the 1000 mg/L chloride concentration contour (right). Given elevations are relative to NAP. The top two plots represent the equilibrium situation, the top middle two the situation for scenario (1): level = 50 cm beneath surface level, the bottom middle two the situation for scenario (2): level = 75 cm beneath surface level and the bottom two the situation for scenario (3): level = 100 cm beneath surface level. All scenario plots represent the situation in the year 2033, after 20 years of infiltration

For the 2D plots it can be seen that water is not only flowing in the South-Eastern direction towards Slimflex F, but water is also flowing in the Western and Eastern directions. Since the brackish ditch lies on top of these contours, freshwater is flowing under the ditch out of the creek ridge. The effect is most dominant in scenario (1) with the highest infiltration flux. The question remains why preferential flowpaths form and why there. This could be due to 'weak spots' in the lithology. If there are holes in confining clay layers then water will preferentially flow into these holes.

8.3.2 Modelled infiltration period

The level controlled drainage system and the pump were installed in May 2013 and water was effectively infiltrating froma period of 2 weeks. The pump was switched on on the 21st of May 2013 and was stopped on the 6th of June due to the lack of water in the ditch where the infiltration water is collected from. This same period has been modelled to look at the accuracy of the model on these short timescales. The year 2013 (up to the 3rd of July) has already been modelled using the daily recharge data. The infiltration experiment has been modelled in a different run and the results of the are compared to the run without infiltration.

The infiltration model run starts on the 1st of April and ends on the 3rd of July. Daily stress periods were used and the daily recharge data from the KNMI was used. The head was controlled for 16 stress periods (21st of May - 6th of June). The stage for infiltration was set at 50 cm beneath surface level. The calculated heads for both the regular 2013 model run (blue graph) as well as the infiltration run (green graph) are given in figure 8.3.3. The infiltration period is inbetween the red dashed lines. When infiltration has stopped, hydraulic heads consist to be elevated for a long period. As of the 3rd of July (the end of the model run), the ground water level has not dropped back to normal levels

yet. This is not what is observed in the monitoring wells. Direct groundwater measurements show a much quicker recovery for the head. Because the head remains elevated for a longer period, water continues to infiltrate for longer than expected. This could lead to an overestimation of the infiltration.

In figures (6.4.1) and (6.4.2) already a freshening of the groundwater at levels 10 m below NAP is measured between the time before infiltration (26-04-2013) and during infiltration (30-05-2013). Whether this results in an increase in the thickness of the freshwater lens remains to be seen, but the model results yield indeed a lowering of the fresh-salt interface by 50 cm (8.3.4 and 8.3.5). The upper graph shows the (elevated) hydraulic head during the infiltration period (red dashed lines), the middle graph shows the normal situation without infiltration and the bottom graph shows the results when infiltration has been implemented in the model.

In figure 8.3.6 the percentual change in water volume compared to today's levels are given for the three scenarios and for values smaller than certain chloride concentration thresholds. The blues lines represent the changes in freshwater volume (water with a chloride concentration smaller than 150 mg/L) which in all scenarios increase drastically. In all cases after 20 years of infiltration, the volume of freshwater in the aquifer has as least doubled (scenario 3) or more than doubled (scenarios 1 and 2). Similar trends are observed for the threshold values of 1000 mg/L and 10000 mg/L. The biggest changes are observed in the first two years after the start of infiltration. For all scenarios the freshwater volume in the aquifer increases by 40 percent within the first two years. Since according to figure 8.2.1 in a worst case scenario (W+) the availability of freshwater decreases by 17 percent in 50 years, the implementation of the level controlled drainage system will be a very good and fast way to cover the freshwater loss by climate change.

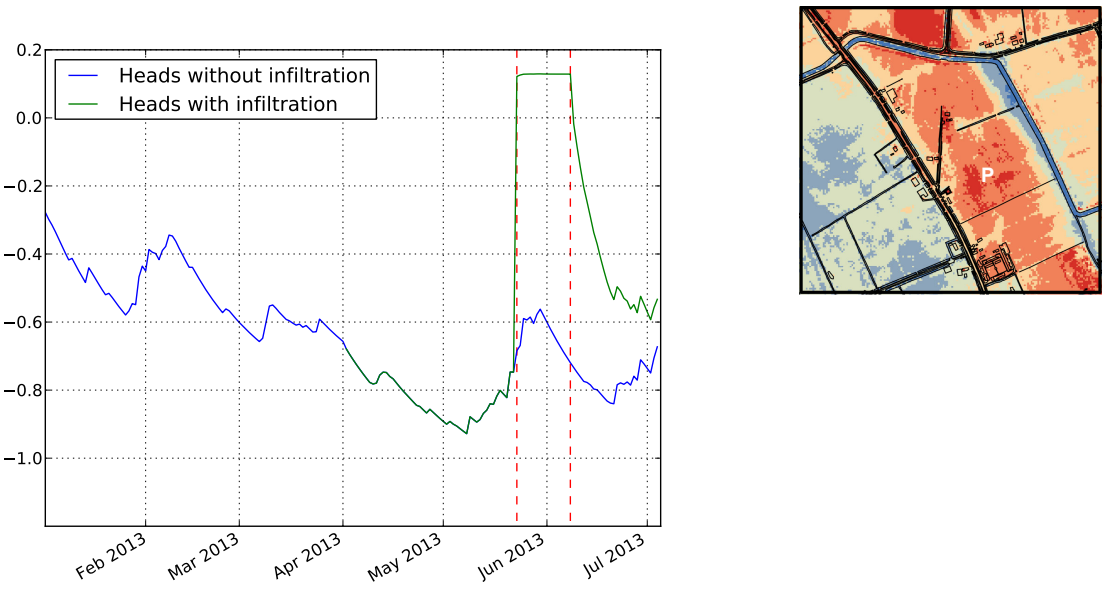

Figure 8.3.3: Modelled hydraulic head without infiltration (blue) and with infiltration (green). The infiltration period is marked inbetween vertical dashed lines.

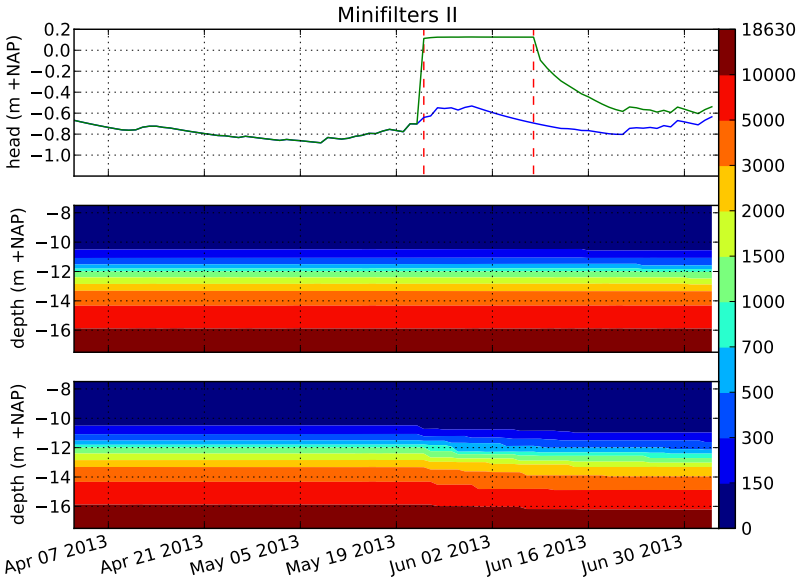

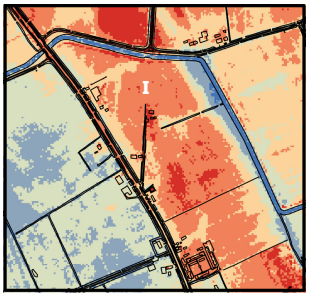

Figure 8.3.4: Minifilters I: timeseries of modelled hydraulic heads (upper graph), chloride concentration (mg/L) without infiltration (middle graph) and chloride concentration (mg/L) including infiltration (lower graph). .

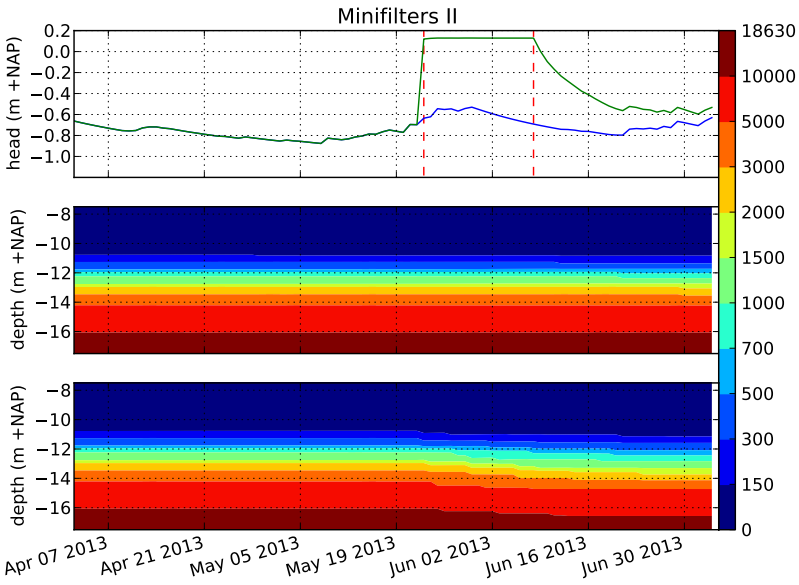

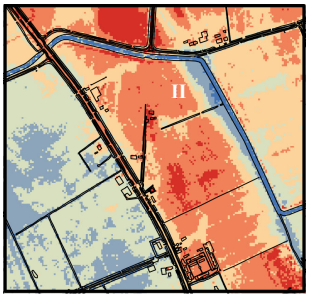

Figure 8.3.5: Minifilters II: timeseries of modelled hydraulic heads (upper graph), chloride concentration (mg/L) without infiltration (middle graph) and chloride concentration (mg/L) including infiltration (lower graph).

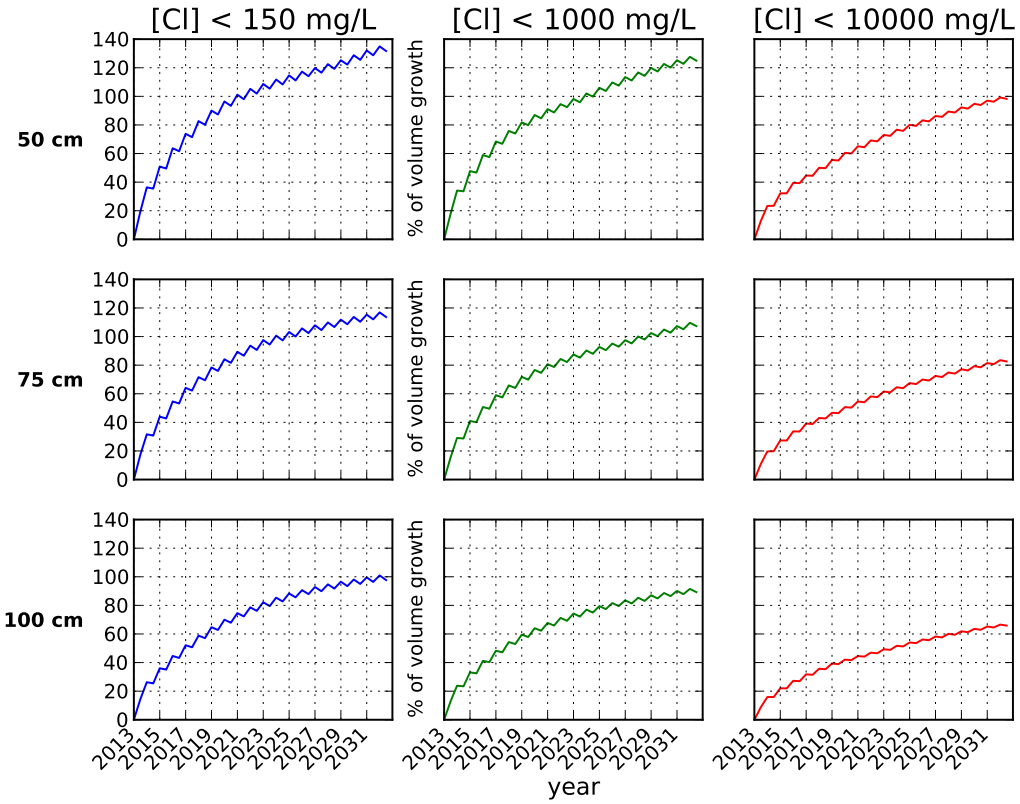

Figure 8.3.6: Percentual changes in water volume for the three levels (50cm, 75 cm and 100 cm below surface level) for 20 years of infiltration. Blue graphs shows all water with chloride concentrations lower than 150 mg/L, green graphs shows all water with chloride concentrations lower than 1000 mg/L and red graphs shows all water with chloride concentrations lower than 10000 mg/L

8.4 MOCDENS3D - SEAWAT comparison

To compare the differences between the model runs, it is important to know the only differences in input values and the solver methods used. The model runs are almost identical. The only differences in parameter input lie in the head closure criterium, which was set to 10^{-5} m for the SEAWAT run, while in the MOCDENS3D 10^{-6} m was used. The value of 10^{-6} m was not possible for the SEAWAT run, because it gave convergence problems. Another difference is that for the SEAWAT run, the HMOC solver method was used. The solver is practically the same as the MOC solver used in MOCDENS3D. The third and final difference lies in the amount of particles used in the SEAWAT and MOCDENS3D runs. Visser [Visser, 2012] did model checks on the relevance of the amount of particles in the simulation. Differences in results between 8 or 27 particles per cell were already very small, so it was chosen to model the SEAWAT run with just 8 particles. This was primarely chosen due to time constraints. For this comparison, the output from the MOCDENS3D run with 8 particles is taken.

The MOCDENS3D - SEAWAT comparison will be done in two parts. In the first part, the results of the yearrun of 2011 in terms of hydraulic head are compared. The results

are given in figure 8.4.1. The modelled heads are nearly identical to the modelled heads in figure 7.4.2. Small differences are present which are most likely not caused numerically, but rather due to the fact that Visser used recharge data from the KNMI measuring station in Vrouwenpolder, while in this study recharge data from Vlissingen has been used.

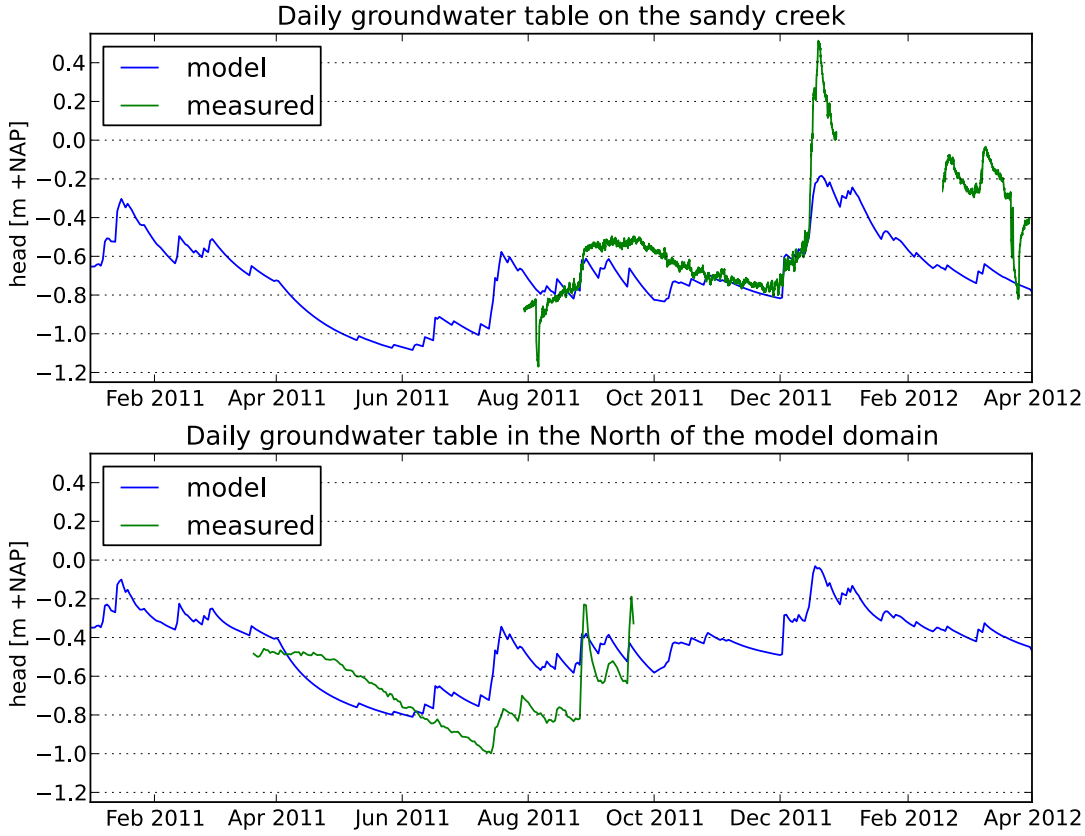

Figure 8.4.1: The year 2011 modelled by the MOCDENS3D code [Visser, 2012].

The other part which is compared is the numerical dispersion calculated by the codes. This will be plotted as the transect of row 90 of the model given in figures 8.4.2 and 8.4.3 for MOCDENS3D and SEAWAT respectively. Again here also minor differences can be seen. The freshwater lens in the creek ridge is 1 meter thicker in the MOCDENS3D run where it reaches to a depth of 14 m compared to the 13 meter in the SEAWAT model. The thickness of the mixing zone is therefore slightly larger for the SEAWAT model. If we would compare the results of the models to the field measurements, the SEAWAT model fits the field measurements better. Apart from the thickness of the freshwater lens, no significant differences between the MOCDENS3D and the SEAWAT model are noticable.

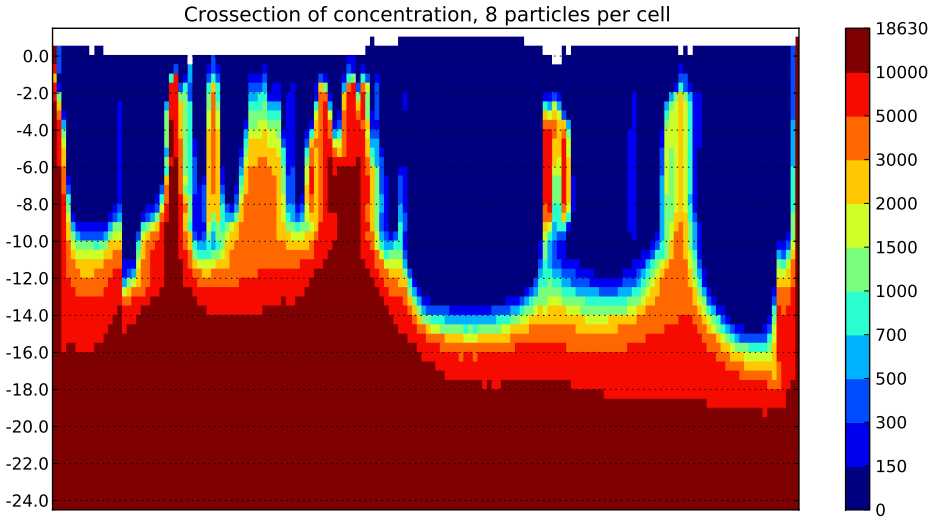

Figure 8.4.2: Chloride concentration (in mg/L) contour plot in row 90 of the MOCDENS3D model of Visser [Visser, 2012]

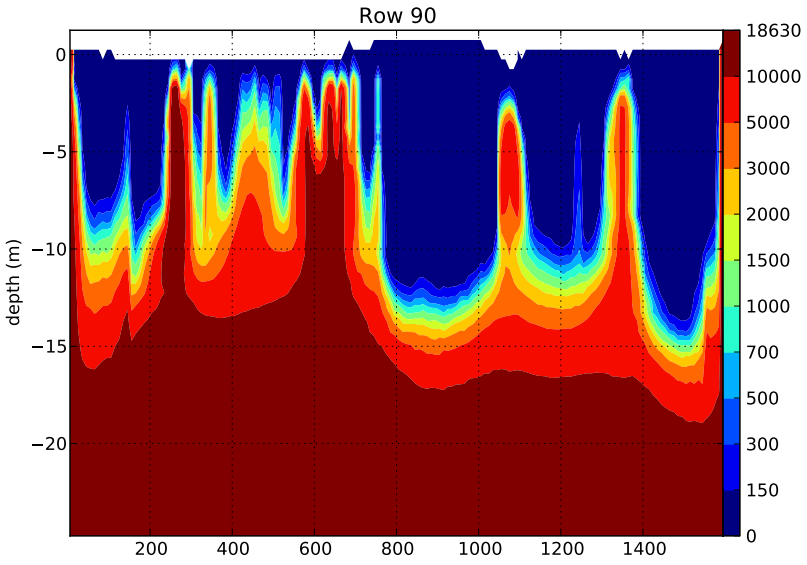

Figure 8.4.3: Chloride concentration (in mg/L) contour plot in row 90 of the SEAWAT model used in this study

9. Discussion

Model calibration

The model has been calibrated using many different, independent measurement techniques and therefore the current day situation is modelled sufficiently well. The thickness of the freshwater lens on the properties of Sanderse and Louwerse has been modelled accordingly to the thickness obtained from the field measurements. Still there are differences between the model and the field measurements. Modelling with stress periods of length half a year give lower hydraulic head values compared to the hourly measurements by divers. This is caused predominantly by the recharge input, which appears to be the dominant factor in this case. This is proved by figure 7.4.1, where the influence of using a crop factor has been shown. For modelling the years 2011, 2012 and 2013, the crop factor has been set to zero. It is debatable whether this is a realistic value, but for the model this works. It is assumed to be reasonable since the groundwater level in summer is so deep (up to 2 meters below surface level), the influence of evaporation can be neglected and the only contributor to groundwater recharge is precipitation.

By using a crop factor of zero, the hydraulic head calculations of both the daily stress period run as well as the weekly stress period run could be fitted well with the diver data for 2011 (figure 7.4.2). Still for the period of December period of 2011, there is still a misfit with the diver data. Calculated hydraulic heads are 60 cm lower than the diver measurements. There could be two explanations. Either MODFLOW is limited in a way that it cannot easily generate large fluctuations in hydraulic head or the recharge data is insufficient. The second explanation is most likely, since recharge data is obtained from the KNMI measuring station in Vlissingen, which is around 15 km from the field site. Locally, rain could have been heavier or peak rains could have caused the steep rise in groundwater level.

For the year 2012 (figure 7.4.3)on the other hand, the calculated heads do not fit with the diver data. This could still be due to the difference in recharge between Vlissingen and Serooskerke. This seems to be the case since the trend in groundwater level remains the same for the model results and the diver data.

Infiltration experiment

The model has been run both on long time scales (stress periods with length of half a year) as well as short time scales (daily stress periods). For the longer time scales, the model is most likely overestimating the infiltration during the winter stress period. Infiltration is modelled to have a constant level throughout the entire halfyear, which is never the case. Many factors influence whether the system can actively infiltrate: (1) fresh water availability in the fresh water ditch, (2) precipitation, (3) problems with the pump and (4) environmental issues for example. During heavy frost in winter, the ditch could be completely frozen and the water cannot be used for infiltration. Periods with large precipitation also are not suitable for infiltration. Although it would be beneficial for water storage, often the soil becomes too wet and water has be released from the aquifer. Mechanical errors in the pump also can temporarely shut down the system. Finally, in August 2013, an sewer spill leaked seewage water in the freshwater ditch of which water is pumped for infiltration. In order to find out that the water was not severely polluted with

chemicals and bacteria, water samples had to be analyzed to verify this. This also shut down the system for several weeks. So although the system might theoretically infiltrate a certain amount of water, in practice the amount will always be less.

Looking at the effect the infiltration in the near future, it seems that the largest gain of freshwater will be gained in the first years of infiltration. This can theoretically explained by the fact that in the beginning of the head difference in the aquifer is greatest. At $t = 0$, the hydraulic head is set to a certain value below surface level h_{level} (in the scenario this was 50 cm, 75 cm or 100 cm). The fresh-brackish interface is found at around 11 m below surface level. Assume the water at the interface to be brackish at interface and the hydraulic head at the interface h_{int}. Apart from the buoyancy effect, the main drive for infiltration is the hydraulic head difference Δh between h_{level} and h_{int}. Several years after infiltration, the fresh-brackish interface will have lowered and the initially brackish water will have been replaced by freshwater. The salt water head (hydraulic head) has changed due to the changes in density and the buoyancy effect has changed as well. The vertical flux q_z will therefore decrease with time. This same effect can also be seen in figure 8.3.1. After every winter infiltration period, the following summer period when no infiltration is occuring, the fresh-brackish interface goes upward again. This effect is strongest in the first years, but becomes less after the system reaches equilibrium again. These results could be verified by continuing the infiltration experiment for a few more years. All 3 scenarios show a lowering of the fresh-brackish interface of 5 meters within the first 4 years. Although this will in reality not be reached, the lens will at least grow a few meters and this is worth monitoring. The model could be further calibrated on the measurements of the coming years.

Another possibility for increasing the accuracy of the infiltration model is to model a few years using weekly or monthly stress periods. In the coming years, the farmers should accurately document the days in which the drainage system is infiltrating. These infiltration times could then be used as input in the model as infiltration stress periods. The precipitation and evaporation data from the KNMI could be used as recharge input. If the depth of the freshwater lens is also monitored in the following years, the model could be further calibrated.

Looking at the effect of infiltration with daily stress periods, the model overestimates the hydraulic head a long time. Groundwater level measurements show that the groundwater level drops much quicker and the 'normal' groundwater level is reached soon after stopping infiltration. The model is therefore less suitable for modelling infiltration on small time scales. This could however be inproved in certain ways. Increasing the hydraulic conductivity of the soil would lower the hydraulic head. Another solution is to devide the already short stress periods into smaller timesteps. The flow equation is solved for every time step in SEAWAT, so the flow equation would be solved more times. This would increase the accuracy of the hydraulic head after infiltration. On the other, this will also increase run time. The final solution would be to increase the *storativity* in the model. MODFLOW does not deal with the unsaturated zone, which is one lacking aspect of the code. This is compensated in the model by simulating the top active cell as an seperate unconfined aquifer and all cells underneath the top active cells as confined cells. The top active cell has then a storativity which is called *specific yield*. The storage capacity in the confined cells is the *elastic storage*. Increasing the elastic storage will increase the water volume expelled from the confined cells when the head in the cell drops.

This will have positive feedback on solving the flow equation. The hydraulic heads in the cells will drop faster.

Climate scenarios

The effects of climate change based on the 4 climate scenarios proposed by the KNMI can be completely compensated by the inplementation of an level controlled drainage system. The maximum reduction in freshwater volume (17 % in 50 years) is seen in climate scenario W+. The minimum gain of freshwater volume is 100 % in 20 years. The needed 17 % is gained already in the first years. The freshwater loss in climate scenario is 7%. In terms of freshwater thickness would this mean a shallowing of the depth to the fresh-brackish interface of 3 meters on the property of Louwerse. On the other hand, the model predicts a freshwater increase for the climate scenarios G and W. If these values are corrected with the Control run, there is no significant freshwater loss of gain in these scenarios. The reason for this lies in the way climate change is modelled. Changes in climate are modelled based solely on the recharge input. Net recharge is calculated from the difference between precipitation and evaporation. For future precipitation, the KNMI had estimates on the actual recharge (in mm precipitation) available for the years 2050. For evaporation, the only information what was available were the percentual increases in evaporation. The values for net precipitation in winter and net evaporation in summer were used as reference values. These values were 1.4 mm/day and -0.2 mm/day respectively. From the data it was found that new recharge rate for winter stress periods changed more compared to the recharge rates for summer stress periods for climate scenarios G and W. For example, the winter recharge rate for scenario G is 1.453 mm/day, while the summer recharge rate was -0.208 mm/day. The recharge rates in winter therefore increase more than the recharge rates are lowering. For the G+ and W+ this is different. Scenario G+ has a winter recharge rate of 1.517 mm/day compared to a summer recharge rate of -0.562 mm/day. From this it can be concluded that recharge input is very important in these climate scenarios. Also the decision on which reference values to use is important.

Comparison MOCDENS3D and SEAWAT

Numerically, MOCDENS3D and SEAWAT are very similar. The difference between the two lies within the fact that MOCDENS3D is based on the MOC3D module, while SEAWAT uses the MT3DMS module. MOC3D supports only the MOC solver for solving the solute transport equation, for MT3DMS more solver methods are available. In this way, SEAWAT is more versatile. Moreover, the possibility of modelling multispecies in SEAWAT is another advantage over MOCDENS3D. Numerically, the codes are comparable. In modelling hydraulic heads, they give the same output since they both use the MODFLOW module for solving the flow equation. Differences between the calculated head data is caused by the fact that Visser used recharge data obtained from the KNMI measuring station at Vrouwenpolder, while for this study the recharge data form the measuring station at Vlissingen had been used.

10. Conclusions

An infiltration experiment has started on a creek ridge near Serooskerke, Walcheren. The goal of the field test was to test the possibility of using a level controlled drainage to increase the size of the freshwater lens in the creek ridge. The field test is located on the properties of two farmers, Werner Louwerse and Johan Sanderse. In the original planning, the experiment was expected to start in late 2012, but due to bad weather conditions and other circumstances, installation of the drainage system could not start until April 2013. The field conditions have been continuously monitored by a wide array of different measurement techniques. The freshwater lens has been monitored in terms of thickness, thickness of the mixing zone and groundwater level.

After several weeks of infiltration, already some freshening at the fresh-brackish interface has been measured. Both the Subsurface Monitoring Device and the EC - measurements on pumped up groundwater show differences in the measurements on 26-04-2013 and 30-05-2013. After a few weeks of infiltration, already the expected change in freshwater lens is measured. Other field measurements show that the freshwater lens on the property of Sanders has an thickness of approximately 10 - 11 m, while the thickness of the freshwater lens on the property of Louwerse is 13 -14 m thick.

The groundwater model has been calibrated to the field measurements and can be used to make predictions on the effectivity of the level controlled drainage system. Although the model gives an overestimation of the evolution of the freshwater lens as a result of infiltration, it is expected that the increase in freshwater volume will be sufficient to counter the loss of freshwater due to the worst climate scenarios proposed by the KNMI. The fastest growth of the freshwater lens is expected to be in the first few years after infiltration has started. The model has also been checked to work on small timescales, but the model gives here an overestimationon the hydraulic head. This will lead to an overestimation in the infiltration as well. Therefore the model is not yet as useful for small timescale predictions.

The comparison between MOCDENS3D and SEAWAT gave no significant differences in terms of numerical dispersion. The main differences lie in the input format and the fact that SEAWAT is more versatile in the solver methods and the ability to model multiple species simultaneously.

Bibliography

[Badon Ghyben, 1888] Badon Ghyben, W., 1888, Nota in verband met de voorgenomen putboring nabij Amsterdam, *Tijdschrift van het Koninklijk Instituut voor Ingenieurs, 5*, 8-22 (Dutch)

[Barlow and Harbaugh, 2006] Barlow, P.M., Harbaugh, A.W., 2006, USGS directions in MODFLOW development, *Groundwater*, 44(6): 771-774

[Emerson and Hedges, 2008] Emerson, S.R., Hedges, J.I., 2008, *Chemical Oceanography and the Marine Carbon Cycle*, University Press Cambridge, ISBN 978-0-521-83313-4

[Fitts, 2002] Fitts, C.R., 2002, *Groundwater Science*, Academic Press: London, Elsevier

[Goes et al., 2009] Goes, B.J.M. Oude Essink, G.H.P. Vernes, R.W. Sergi, F., 2009, Estimating the depth of fresh and brackish groundwater in a predominantly saline region using geophysical and hydrological methods, Zeeland, the Netherlands, *Near Surface Geophysics*, p. 401-412, 2009.

[Guo and Langevin, 2002] Guo, W., Langevin, C.D., 2002, User's guide to SEAWAT: A computer program for simulation of three-dimensional variable-density ground-water flow, *United States Geologival Survey*

[Jacobs, 2013] Jacobs, A.F.W., 2013, Calibration and employability of the EM-Slimflex, *Deltares internal report*

[Konikow and Bredehoeft, 1978] Konikow, L.F., Bredehoeft, J.D., 1978, Computer model of two-dimensional solute transport and dispersion in ground water: *U.S. Geological Survey Techniques of Water-Resources Investigations*, Book 7, Chapter C2, 90 p.

[Konikow and Goode, 1996] Konikow, L.F., Goode, D.J., Hornberger, G.Z., 1996, A Three- Dimensional Method-of-Characteristics Solute-Transport Model (MOC3D): *U.S. Geological Survey Water-Resources Investigations Report* 96-4267, 87 p.

[Langevin and Guo, 2002] Langevin, C.D., Guo, W., 2002, User's guide to SEAWAT: a computer program for simulation of three-dimensional variable-density ground-water flow, *USGS report*

[Langevin and Guo, 2006] Langevin, C.D., Guo, W., 2006, MODFLOW/MT3DMS-based simulation of variable-density ground water flow and transport, *Groundwater*, 44(3): 339-351

[de Louw et al., 2011] de Louw, P.G.B., Eeman, S., Siemon, B., Voortman, R., Gunnink, J., van Baaren, E.S. et al., 2011, Shallow rainwater lenses in deltaic areas with saline seepage *Hydrology and Earth System Sciences Discussions*

[Oude Essink, 2001] Oude Essink, G.H.P., 2001, Saltwater intrusion in 3D Large-Scale Aquifers: A Dutch Case, *Phys. Chem Earth*, 26(4): 337-344

[Oude Essink, 1999] Oude Essink, G.H.P., 1999, Simulating 3D density dependent groundwater flow: the adapted MOC3D, *Proceeding SWIM 15, Ghent, Belgium*

[Pauw, 2012] Pauw, P., 2012, Overview of common field measurements: applicable in the research on freshwater lenses in coastal areas, *Deltares report*

[Post, Kooi and Simmons, 2007] Post, V., Kooi, H., Simmons, C., 2007, Using hydraulic head measurements in variable-density ground water flow analyses, *Groundwater*, 45: 664-671

[Stuyfzand, 1986] Stuyfzand, P.J., 1986, A new hydrochemical classification of water-types: principles and application to the coastal dunes aquifer system of the Netherlands, *Netherlands Journal of Geosciences*, 90(4), 293-310

[van Bakel et al., 2008] van Bakel, P.J.T., van Boekel, E.M.P.M., Noij, I.G.A.M., 2008, Modelonderzoek naar effecten van conventionele en samengestelde, peilgestuurde drainage op de hydrologie en nutrintenbelasting (Dutch), *Alterra-report 1647*, ISSN 1566-7197

[van Betuw, 1952] van Betuw, T.W.J. ,1952, De bodemkartering van Nederland, deel XII: De bodemkartering van Walcheren. Verslagen landbouwkundige onderzoekingen nr 58.4, Stichting bodemkartering (Dutch)

[van Baaren et al., 2012] van Baaren, E.S., Oude Essink, G.H.P., Janssen, G.M.C.M., de Louw, P.G.B., Heerdink, R., Goes, B., 2012, Verzoeting/verzilting freatisch grondwater in de provincie Zeeland, rapportage 3D dichtheidsafhankelijk grondwatermodel, *Deltares* (Dutch)

[van Meerten, 1986] van Meerten, J.J., 1986, Kunstmatige infiltratie in kreekruggen (Dutch), *TH Delft Report*

[Vos and van Heeringen, 1997] Vos, P.C., van Heeringen, R.M., 1997, Holocene geology and occupation history of the province of Zeeland, *Mededelingen Nederlands Instituut voor Toegepaste Geowetenschappen TNO 59*, NITG-TNO, Utrecht, 5-109

[Visser, 2012] Visser, M., 2012, MSc thesis: Aquifer storage and recovery in a fossil creek bed; managing droughts in a brackish environment, *Utrecht University and Deltares*

[Voortman, 2010] Voortman, B., 2010, De invloed van gebiedseigenschappen en klimaatverandering op de dikte en vorm van regenwaterlenzen in de Provincie Zeeland, Een 3D modelstudie op perceelschaal (Dutch), *Deltares report*

[Werner and Simmons, 2009] Werner, A.D., Simmons, C.T., 2009, Impact of Sea-Level Rise on Sea Water Intrusion in Coastal Aquifers, *Groundwater*, 47(2): 197-204

[Zheng and Bennet, 1995] Zheng, C., and Bennett, G.D., 1995, *Applied contaminant transport modeling, theory and practice*, Van Nostrand Reinhold, 440 p.

[Zheng and Wang, 1998] Zheng, C., Wang, P.P., 1998, MT3DMS: A Modular Three-Dimensional Multispecies Transport Model, *Documentation and User's Guide*

11. Appendix

1. Enlargement of figure 5.1.1. Locations of CVES profiles measured in October 2012

2. Enlargement of figure 5.2.1. Locations of the monitoring wells (white numbers) within the model domain (edge). The locations are coded conform the code given to the monitoring well in table 5.2.1. At locations I (Minifilters I), III (Minifilters III) and E (Slimflex E) the borehole analysis is measured in the same borehole as the Slimflex measurements. At location II, Minifilters II is situated. The borehole analysis is done in the borehole of the Subsurface Monitoring Device which is located 5 m west of II.

3. Borehole log of Minifilters I/Slimflex A. Coordinates of the borehole log are x = 30074.5, y = 398192.5

4. Borehole log of SMD/Slimflex B. Coordinates of the borehole log are x = 30126.2, y = 398190.3

5. Borehole log of Minifilters III/Slimflex C. Coordinates of the borehole log are x = 30226.4, y = 398185.6

6. Borehole log of Slimflex E. Coordinates of the borehole log are x = 30176.2, y = 398076.8